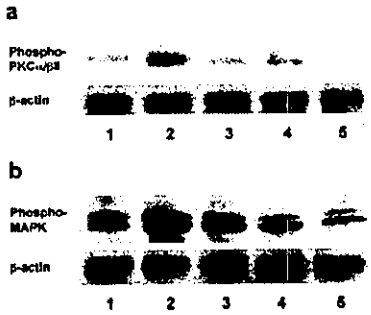

FIG. 10. **Effects of inhibitors on MIF-induced phosphorylation of PKC and MAPK.** Phosphorylation of PKCα/βII and MAPK in dermal fibroblasts induced by MIF was examined in the presence of various inhibitors against PKC and tyrosine kinases. *a*, MIF-induced PKC phosphorylation was measured at 60 min in the presence or absence of tyrosine kinase inhibitors, PP2, genistein, and herbimycin A. Western blot analysis of the cell lysates (40 μg) was carried out using a phospho-PKCα/βII antibody. *Lane 1*, control; *lane 2*, MIF 100 ng/ml; *lane 3*, MIF 100 ng/ml + PP2 10 μM; *lane 4*, MIF 100 ng/ml + genistein 100 μM; *lane 5*, MIF 100 ng/ml + herbimycin A 10 μM. Western blot analysis for β-actin is shown as a control. *b*, MIF-induced MAPK phosphorylation was evaluated at 60 min in the presence or absence of tyrosine kinase inhibitors (genistein, herbimycin A), and PKC inhibitor GF109203X. *Lane 1*, control; *lane 2*, MIF 100 ng/ml; *lane 3*, MIF 100 ng/ml + genistein 100 μM; *lane 4*, MIF 100 ng/ml + herbimycin A 10 μM; *lane 5*, MIF 100 ng/ml +GF109203X 10 μM. Western blot analysis for β-actin is shown as a control.

ation of PKC and MAPK induced by MIF (100 ng/ml) for 60 min. We found that the MIF-induced increase in the phosphorylation of PKC and MAPK was suppressed by transfection of CSK plasmid, whereas CSK^- plasmid had no significant effect (Fig. 11).

DNA Binding Activity of AP-1 in Response to MIF—By using the AP-1 consensus oligonucleotide, the DNA binding activities of AP-1 were examined after MIF stimulation (100 ng/ml). The DNA binding activities of AP-1 were significantly up-regulated for up to 120 min. The binding activity was significantly down-regulated with the addition of an excessive amount of non-labeled AP-1 oligonucleotide (100-fold) (Fig. 12).

DISCUSSION

The effects of sunlight have fascinated researchers for decades because nearly every living organism on earth is likely to be exposed to sunlight, including its ultraviolet (UV) fraction it. Among sunlight's detrimental long term effects is skin photoaging, which is a well-documented consequence of exposure to UVA and UVB radiation. Photoaged skin is biochemically characterized by a predominance of abnormal elastic fibers in the dermis and by a dramatic decrease in distinct collagen types. MMPs are crucial factors involved in the connective tissue remodeling accompanying ultraviolet radiation-induced skin damage.

MIF functions as a pleiotropic cytokine by participating in inflammation and immune responses. MIF was originally discovered as a lymphokine involved in delayed hypersensitivity and various macrophage functions, including phagocytosis, spreading, and cell growth activity (22–24). MIF was recently reevaluated as a proinflammatory cytokine and pituitary-derived hormone that potentiates endotoxemia (25). This protein is ubiquitously expressed in various organs, including the skin, brain, and kidney (27–33). In the skin, MIF is expressed in the epidermis, particularly in the basal layer (15).

Premature aging of the skin secondary to chronic exposure to UV radiation is primarily due to qualitative and quantitative changes in the dermal extracellular matrix, resulting in increased fragility, reduced recoil capacity, blister formation, and impaired wound healing. Interstitial collagens, the major

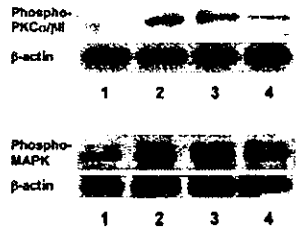

FIG. 11. **Effects of CSK and CSK^- on MIF-induced phosphorylation of PKC and MAPK.** Phosphorylation of PKCα/βII and MAPK in dermal fibroblasts by MIF for 60 min was examined by transfection of CSK and CSK^- plasmid. Western blot analysis of the cell lysates (40 μg) was carried out using phospho-PKCα/βII and phosphoMAPK antibodies. *Lane 1*, control; *lane 2*, MIF 100 ng/ml; *lane 3*, MIF 100 ng/ml +CSK^-, *lane 4*, MIF 100 ng/ml+ CSK. We performed Western blot analysis for β-actin as a control.

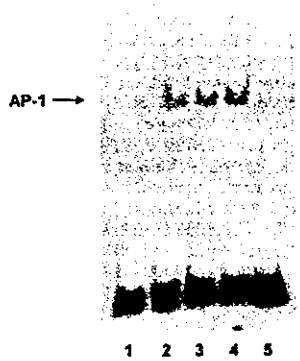

FIG. 12. **EMSA of AP-1 binding activity by MIF stimulation.** Dermal fibroblasts were stimulated with MIF (100 ng/ml) at the indicated times. Nuclear extracts were prepared, and the AP-1 DNA-binding activity was analyzed by EMSA. *Lane 1*, free probe labeled AP-1 binding oligonucleotide without nuclear extracts; *lane 2*, MIF at 0 min; *lane 3*, MIF at 60 min; *lane 4*, MIF at 120 min; *lane 5*, cold AP-1 oligonucleotide (100-fold excess).

structural components of the dermis, have been found to be particularly diminished in actinically damaged skin. Although there is a direct role for human dermal fibroblasts and an indirect participation of epidermal keratinocytes in MMP-1 production after UVB irradiation, UVA irradiation is known to reach the reticular dermis, rendering fibroblasts possible targets. Recent studies have shown that UV irradiation significantly affects the coordinated regulation of various MMPs and TIMPs (2). The expression of MMPs is regulated at a transcriptional level by various cytokines and other mediators in both a positive and negative manner under certain physiological conditions. Moreover, the enzyme activities of MMPs are post-transcriptionally controlled by activation of latent proenzymes as well as by interactions with their specific inhibitors, referred to as TIMPs.

It has been reported that the biosynthesis of MMP-1 is up-regulated by 12-*O*-tetradecanoylphorbol-13-acetate (TPA), cytokines, and growth factors such as IL-1, TNF-α, IL-6, epidermal growth factor, and platelet-derived growth factor, in a variety of cells, including fibroblasts. In contrast, transforming growth factor-β, retinoic acid, and dexamethasone down-regulate MMP-1 (34). We have recently demonstrated that MIF expression is significantly up-regulated by growth factors such as TGF-β and PDGF (35). These findings indicate that the mRNA of metalloproteinases may be precisely regulated through a complex mechanism that includes both growth factors and cytokines. UVA irradiation of human dermal fibroblasts was found to elicit an increase in specific quantities of mRNA and the bioactivities of the cytokines IL-1α and IL-1β; it

then induced interrelated IL-1 autocrine feedback loops, ultimately leading to tissue degradation in photoaging. Singlet oxygen is an early intermediate in the signaling pathway of IL-1-mediating UVA induction of interstitial collagenase. IL-1α and IL-1β may, at least in part, cause the imbalance between MMPs and TIMPs. For example, there have been reports that the generation of singlet oxygen and other reactive oxygen species precedes the induction of IL-1 (36).

We have here demonstrated that UVA stimulation leads to a significant increase in specific MIF mRNA and protein levels in human dermal fibroblasts. This remarkable increase in MIF occurred by UVA irradiation at intensities above 2 J/cm^2. We also found that IL-1α and IL-1β up-regulate MIF (data not shown). Furthermore, it was found that MIF has the potential to stimulate IL-1β production. Constitutive collagenase synthesis has been reported to be regulated by an IL-1β autocrine mechanism (36). In this study, we demonstrated that anti-MIF neutralizing antibody suppresses the expression of MMP-1 induced by UVA. It is therefore possible that UVA irradiation may stimulate MIF production by an autocrine loop of both MIF and IL-1. MIF up-regulates MMP-1 mRNA as well as protein levels and MMP-1 activity by zymography in dermal fibroblasts. In contrast, TIMP-1 is slightly up-regulated by MIF.

In the present study, we also demonstrated that protein expression of MMP-13 is significantly decreased compared with the levels in control WT-mice after UVA irradiation (10 J/cm^2). In the rodent, regulation of MMP-13 most likely plays an important role in extracellular matrix degradation. These results indicate that MIF-deficient skin especially fibroblasts produce less MMP-13 after UVA irradiation. We therefore hypothesize that MIF participates in the production of MMP-13 and is a significant factor in the degradation of the extracellular matrix in the dermis.

The molecular mechanisms of UV-induced MMPs have yet to be defined. UV-induced expression of pro-inflammatory cytokines such as IL-1β and TNF-α may also in part account for the expression of MMPs. IL-1β-induced expression of MMP-1 is mediated by transactivation of the EGF receptor and through an ERK pathway in human keratinocytes. Collagenase synthesis by fibroblasts and keratinocytes involves the PKC second-messenger system, and corticosteroids have been shown to suppress its synthesis at the level of gene transcription. Long-wavelength UV light (UVA, 320–400 nm) stimulates the synthesis of interstitial collagenase and increases PKC activity in human skin fibroblasts *in vitro*. Ultraviolet irradiation activates growth factor and cytokine receptors on keratinocytes and dermal cells, resulting in downstream signal transduction through an activation of MAP kinase pathways. These signaling pathways converge in the nucleus of cells to induce c-Jun, which heterodimerizes with the constitutively expressed c-Fos to form activated complexes of the transcription factor AP-1. In the dermis and epidermis, AP-1 induces the expression of the matrix metalloproteinases, such as collagenase, 92-kDa gelatinase, and stromelysin, which degrade collagen and other proteins that comprise the dermal extracellular matrix. It has been reported that MIF induces MMP-1 via tyrosine kinase-, PKC-, and AP-1-dependent pathways in synovial fibroblasts in patients with rheumatoid arthritis (34). Consistent with this finding, we showed that the DNA binding activity of AP-1 was up-regulated by MIF stimulation. Furthermore, a JNK inhibitor blocks the activation of c-Jun and has no effect on p38 and MAPK activities (37, 38). In the present study, we observed a reduction in the MMP-1 mRNA level using a specific JNK inhibitor. Therefore, it is conceivable that activation of c-Jun plays an important role in the signal transduction pathway of MIF-induced MMP-1 expression.

Furthermore, we demonstrated that protein kinase C, raf, and MAPK were phosphorylated, but p38 was not phosphorylated in the same manner. Activation of PKC is one of the earliest events in the cascade leading to a variety of cellular responses. There are multiple PKC isoforms, including classical PKCs (α, βI, βII, and γ), which bind calcium, diacylglycerol (DAG) and phospholipids; novel PKCs (δ, ϵ, η, and θ), which are regulated by DAG and phospholipids; and atypical PKCs: ζ and λ, which lack calcium- or DAG-binding domains. Human dermal fibroblasts are known to express α, δ, ϵ, and ζ isoforms of PKC. Among them, PKCα is thought to be the dominant isoform in the fibroblasts (26). By MIF stimulation, we showed the phosphorylation of PKCα/βII and δ occurred, but not that of PKCζ/λ, suggesting that activation of PKCα or δ can play an important role in MIF signal transduction. CSK has been reported to phosphorylate the carboxyl tyrosine residues of Src family tyrosine kinases and inhibit their functions (17). Using CSK and a kinase-negative mutant of CSK (CSK$^-$) in addition to chemical inhibitors, phosphorylation of PKC and MAPK by MIF stimulation was suppressed by CSK, genistein, and herbimycin A. These facts strongly suggest that PKC and MAPK activation depends on activation of Src family tyrosine kinases.

In conclusion, MIF was found to be up-regulated by UVA irradiation in association with IL-1 in human dermal fibroblasts. Upon MIF stimulation, PKC, Raf, and MAPK can be activated in dermal fibroblasts, and up-regulation of the DNA-binding activity of AP-1 might also take place. Clinically, it has been reported that MIF is closely related to the exacerbation of a variety of diseases, including autoimmune diseases, allergic disease, and carcinogenesis. Hence, this newly identified mechanism may contribute to our understanding of photo-induced dermal connective tissue damage, which results in photoaging. These findings are promising for the potential of MIF inhibitors for therapeutic use in patients with severe photodamage related disorders.

Acknowledgment—We thank Ayumi Honda for technical assistance.

REFERENCES

1. Ohnishi, Y., Tajima, S., Akiyama, M., Ishibashi, A., Kobayashi, R., and Horii, I. (2000) *Arch. Dermatol. Res.* **292,** 27–31
2. Fisher, G. J., Wang, Z. Q., Datta, S. C., Varani, J., Kang, S., and Voorhees, J. J. (1997) *N. Engl. J. Med.* **337,** 1419–1428
3. Brenneisen, P., Oh, J., Wlaschek, M., Wenk, J., Briviba, K., Hommel, C., Herrmann, G., Sies, H., and Scharffetter-Kochanek, K. (1996) *Photochem. Photobiol.* **64,** 877–885
4. Brauchle, M., Gluck, D., Di Padova, F., Han, J., and Gram, H. (2000) *Exp. Cell Res.* **258,** 135–144
5. Alexander, J. P., and Acott, T. S. (2001) *Invest. Ophthalmol. Vis. Sci.* **42,** 2831–2838
6. Wlaschek, M., Heinen, G., Poswig, A., Schwarz, A., Krieg, T., and Scharffetter-Kochanek, K. (1994) *Photochem. Photobiol.* **59,** 550–556
7. Rutter, J. L., Benbow, U., Coon, C. I., and Brinckerhoff, C. E. (1997) *J. Cell. Biochem.* **66,** 322–336
8. Kawaguchi, Y., Tanaka, H., Okada, T., Konishi, H., Takahashi, M., Ito, M., and Asai, J. (1996) *Arch. Dermatol. Res.* **288,** 39–44
9. David, J. R. (1966) *Proc. Natl. Acad. Sci. U. S. A.* **56,** 72–77
10. Bloom, B. R., and Bennett, B. (1966) *Science* **153,** 80–82
11. Nishihira, J. (1998) *Int. J. Mol. Med.* **2,** 17–28
12. Bucala, R. (1996) *FASEB J.* **10,** 1607–1613
13. Nishihira, J. (2000) *J. Interferon. Cytokine. Res.* **20,** 751–762
14. Herrmann, G., Wlaschek, M., Lange, T. S., Prenzel, K., Goerz, G., and Scharffetter-Kochanek, K. (1993) *Exp. Dermatol.* **2,** 92–97
15. Shimizu, T., Ohkawara, A., Nishihira, J., and Sakamoto, W. (1996) *FEBS Lett.* **381,** 199–202
16. Nishihira, J., Kuriyama, T., Sakai, M., Nishi, S., Ohki, S., and Hikichi, K. (1995) *Biochim. Biophys. Acta* **1247,** 159–162
17. Sabe H., Hata A., Okada M., Nakagawa H., Hanafusa H. (1994) *Proc. Natl. Acad. Sci. U. S. A.* **91,** 3984–3988
18. Honma, N., Koseki, H., Akasaka, T., Nakayama, T., Taniguchi, M., Serizawa, I., Akahori, H., Osawa, M., and Mikayama, T. (2000) *Immunology* **100,** 84–90
19. Shimizu, T., Abe, R., Ohkawara, A., Mizue, Y., and Nishihira, J. (1997) *Biocem. Biophys. Res. Commun.* **240,** 173–178
20. Yu, W., Woessner, F., Jr. (2001) *Anal. Biochem.* **293,** 38–42
21. Cano, E., Mahadevan, L. (1995) *Trends Biochem. Sci.* **20,** 117–122
22. Adachi, O., Kawai, T., Takeda, K., Matsumoto, M., Tautsui, H., Sakagami, M.,

Nakanishi, K., and Akira, S. (1998) *Immunity* **9**, 143–150
23. Nathan, C. F., Karnovsky, M. L., and David, J. R. (1971) *J. Exp. Med.* **133**, 1356–1376
24. Churchill, W. H., Jr., Piessens, W. F., Sulis, C. A., and David, J. R. (1975) *J. Immunol.* **115**, 781–786
25. Nishino, T., Bernhagen, J., Shiiki, H., Calandra, T., Dohi, K., and Bucala, R. (1995) *Mol. Med.* **1**, 781–788
26. Choi, S. W., Park, H. Y., Rubeiz, N. G., Sachs, D., and Gilchrest, B. A. (1998) *J. Dermatol. Sci.* **18**, 54–63
27. Suzuki, T., Ogata, A., Tashiro, K., Nagashima, K., Tamura, M., and Nishihira, J. (1999) *Brain. Res.* **816**, 457–462
28. Lan, H. Y., Yang, N., Brown, F. G., Isbel, N. M., Nikolic-Paterson, D. J., Mu, W., Metz, C. N., Bacher, M., Atkins, R. C., and Bucala, R. (1998) *Transplantation* **66**, 1465–1471
29. Lan, H. Y., Mu, W., Yang, N., Meinhardt, A., Nikolic-Paterson, D. J., Ng, Y. Y., Bacher, M., Atkins, R. C., and Bucala, R. (1996) *Am. J. Pathol.* **149**, 1119–1127
30. Imamura, K., Nishihira, J., Suzuki, M., Yasuda, K., Sasaki, S., Kusunoki, Y., Tochimaru, H., and Takekoshi, Y. (1996) *Biochem. Mol. Biol. Int.* **40**, 1233–1242
31. Tesch, G. H., Nikolic-Paterson, D. J., Metz, C. N., Mu, W., Bacher, M., Bucala, R., Atkins, R. C., and Lan, H. Y. (1998) *J. Am. Soc. Nephrol.* **9**, 417–424
32. Bacher, M., Meinhardt, A., Lan, H. Y., Dhabhar, F. S., Mu, W., Metz, C. N., Chesney, J. A., Gemsa, D., Donnelly, T., Atkins, R. C., and Bucala, R. (1998) *Mol. Med.* **4**, 217–230
33. Nishibori, M., Nakaya, N., Tahara, A., Kawabata, M., Mori, S., and Saeki, K. (1996) *Neurosci. Lett.* **213**, 193–196
34. Onodera, S., Kaneda, K., Mizue, Y., Koyama, Y., Fujinaga, M., and Nishihira, J. (2000) *J. Biol. Chem.* **275**, 444–450
35. Takahashi N., Nishihira J., Sato Y., Kondo M., Ogawa H., Ohshima T., Une Y., and Todo S. (1998) *Mol. Med.* **4**, 707–714
36. Wlaschek, M., Wenk, J., Brenneisen, P., Briviba, K., Schwarz, A., Sies, H., and Scharffetter-Kochanek, K. (1997) *FEBS Lett.* **413**, 239–242
37. Bonny, C., Oberson, A., Negri, S., Sauser, C., and Schorderet, D. F. (2001) *Diabetes* **50**, 77–82
38. Bennett, B. L., Sasaki, D. T., Murray, B. W., O'Leary, E. C., Sakata, S. T., Xu, W., Leisten, J. C., Motiwala, A., Pierce, S., Satoh, Y., Bhagwat, S. S., Manning, A. M., and Anderson, D. W. (2001) *Proc. Natl. Acad. Sci. U. S. A.* **98**, 13681–13686

Fas-disabling small exocyclic peptide mimetics limit apoptosis by an unexpected mechanism

Akihiro Hasegawa*†, Xin Cheng*†, Kiichi Kajino*, Alan Berezov*, Kaoru Murata‡, Toshinori Nakayama‡, Hideo Yagita§, Ramachandran Murali*¶, and Mark I. Greene*¶

*Department of Pathology and Laboratory Medicine, Abramson Family Cancer Research Institute, University of Pennsylvania School of Medicine, 252 John Morgan Building, 36th and Hamilton Walk, Philadelphia, PA 19104-6082; ‡Department of Molecular Immunology, Graduate School of Medicine, Chiba University, Chiba 260-8670, Japan; and §Department of Immunology, Juntendo University School of Medicine, Tokyo 113-8421, Japan

Communicated by Peter C. Nowell, University of Pennsylvania School of Medicine, Philadelphia, PA, March 10, 2004 (received for review December 12, 2003)

Fas ligand- (FasL) mediated apoptosis is an important element of tissue-specific organ damage. We have developed biologically active small exocyclic peptide mimetics that disable apoptotic functions of Fas. The most effective mimetic binds to both its receptor and FasL with comparable affinity. *In vitro*, the most effective antagonist blocked FasL-induced cytotoxicity completely and specifically. *In vivo*, the antagonistic mimetic also prevented Concanavilin A (Con A) induced hepatitis, a $CD4^+$ T cell-mediated animal model of liver injury. Although current approaches prevent Fas receptor signaling by excluding FasL binding to Fas, the small molecule mimetics reported here disable Fas by promoting a defective Fas–FasL receptor complex. This event desensitizes FasL-mediated apoptosis by inhibiting extracellular signal regulated kinase activity and up-regulating NF-κB.

Inhibitor | rational drug design

Fas (CD95/APO-1) and its specific ligand [Fas ligand (FasL)/CD95L] are members of the tumor necrosis factor receptor (TNFR) and TNF families of proteins, respectively (1). The interaction between Fas and FasL triggers a cascade of subcellular events that results in a definable cell death process in Fas-expressing targets. Fas is a 45-kDa type I membrane protein expressed constitutively in various tissues, including spleen, lymph nodes, liver, lung, kidney, and ovary (2). FasL is a 40-kDa type II membrane protein, and its expression is predominantly restricted to lymphoid organs and perhaps certain immune-privileged tissues (3). In humans, FasL can induce cytolysis of Fas-expressing cells, as either a membrane-bound or a 17-kDa soluble form, which is released through metalloproteinase-mediated proteolytic shedding (4, 5). The FasL/Fas system has been implicated in the control of immune response and inflammation and response to infection, neoplasia, and death of parenchymal cells in several organs (1, 6, 7). Defects of the FasL/Fas system can limit lymphocyte apoptosis and lead to lymphoproliferation and autoimmunity (8).

Concanavilin A (Con A) induced hepatitis is an experimental murine model of human autoimmune hepatitis (9). T cell activation plays a crucial role in the process of Con A-induced hepatitis (9, 10). Hepatic injury seems to be induced by several different mechanisms involving Fas-FasL (11–13), the perforin-granzyme system (14), IFN-γ (12), and TNF-α-mediated cytotoxicity (10, 15–18). Hepatic damage depends primarily on the Fas-FasL system, because FasL-defective *gld/gld* mice or Fas-defective *lpr/lpr* mice are resistant to liver injury induced by Con A treatment (12, 13).

Macromolecules such as monoclonal anti-FasL antibody and recombinant soluble Fas protein are potential candidate antagonists for clinical studies (19, 20).

Peptidomimetics that are constructed to resemble secondary structural features of the targeted protein represent an approach to overcome some of the limitations of macromolecules and can mimic inhibitory features of large molecules such as antibody (21) and soluble receptors (21, 22).

We found that a potent small molecular species we have developed is specific to Fas and may lead to the formation of defective receptor ensembles. The molecular and biological features suggest that the previously undescribed mimetics may have therapeutic applications in disease states mediated by Fas.

Experimental Protocol

Materials. Human recombinant TNF-α was obtained from Roche Diagnostics. Flag-tagged soluble human Fas ligand (FasL-Flag) and human Fas extra cellular domain-IgGFc fusion protein (Fas-Fc) were purchased from Kamiya Biomedical (Seattle). Human recombinant TNFR (type 1) extracellular domain-IgGFc fusion protein was obtained from R & D Systems. Anti-Flag-horseradish peroxidase antibody, hydrogen peroxide solution, 3, 3′, 5 ,5′-tetramethylbenzidine, and Con A were from Sigma.

Cell Line. American Type Culture Collection Jurkat cells were grown in RPMI medium 1640 supplemented with 10% heat inactivated FCS/L-glutamine (2 mM)/penicillin (100 units/ml)/streptomycin (100 μg/ml) at 37°C in a humidified 5% CO_2 atmosphere.

Mice. Eight-week-old C57BL/6 (B6) mice were purchased from CLEA Japan (Tokyo). All mice used were maintained under specific pathogen-free conditions in our animal facility.

Molecular Modeling. Computer modeling and structural analysis were performed by using both QUANTA and INSIGHT (Molecular Simulations, San Diego). The molecular model of the human Fas–FasL complex was built by using the crystal structure of the TNFR and the molecular model of Fas (23) as described (24).

Peptide Synthesis and Cyclization. Peptides were synthesized and purified by the Chemistry Laboratory of the University of Pennsylvania. The peptides containing internal cysteine residues were refolded, oxidized, and purified as described (22).

Solid-Phase Ligand-Binding Assay. Binding of Flag-tagged soluble FasL and peptide to Fas was determined by using the standard solid-phase binding assay by using ELISA (25). Briefly, the Fas-Fc fusion protein (250 ng/ml) was immobilized onto a 96-well ELISA plate (Costar). After blocking and subsequent washing, Flag-tagged soluble FasL (100 ng/ml) peptide was added to the Fas-Fc for 2 h. The plate was washed and incubated with anti-FLAG(M2) for 1-h washes, and horseradish peroxidase antibody was added for 1 h. Finally, the plate was washed, and the enzyme reaction was started. Absorbance at 450 nm was measured with an ELISA reader.

Biosensor Analysis. All experiments were carried out on a BIAcore 3000 instrument (Biacore, Uppsala, Sweden) as described (26).

Abbreviations: FasL, Fas ligand; ERK, extracellular regulated kinase; JNK, c-jun N-terminal kinase; TNF, tumor necrosis factor; TNFR, TNF receptor.

†A.H. and X.C. contributed equally to this work.

¶To whom correspondence may be addressed. E-mail: murali@xray.med.upenn.edu or greene@reo.med.upenn.edu.

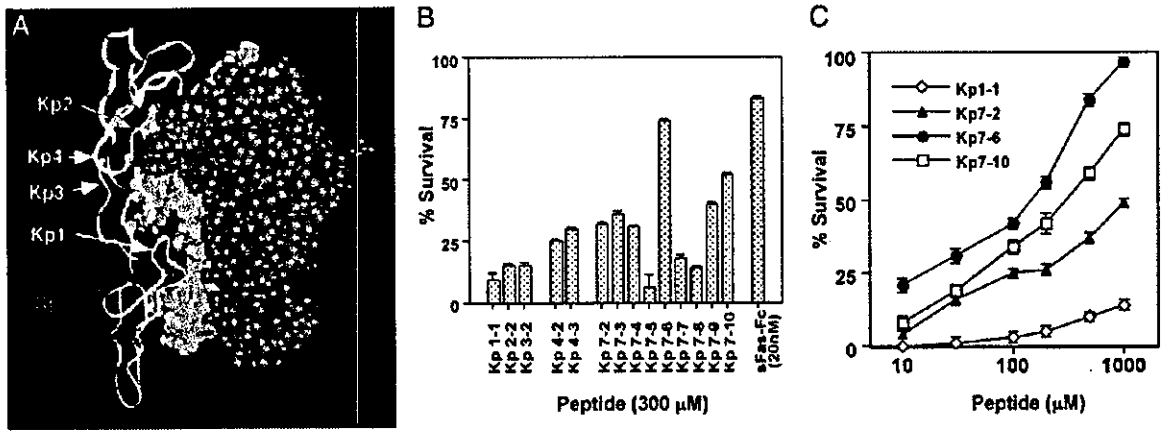

Fig. 1. Identification of FasL inhibitor. (*A*) Molecular model and 3D structure of the critical binding site in the FasL–Fas complex. Molecular interaction analyses between FasL and Fas identified the major sites of interaction that are shown; monomeric Fas (gray), dimeric FasL (green and violet), Kp1 (yellowish green), Kp2 (pink), Kp3 (blue), Kp4 (turquoise), and Kp7 (red). (*B*) Inhibition of FasL binding to the Fas receptor by exocyclic peptidemimetics in a binding assay. Inhibition activities of several mimetics from different regions were compared at 300 nM each peptide and 20 nM soluble Fas receptor. Inhibition (%) by several doses of peptides was calculated and plotted. The results represent the means and standard deviations derived from three independent experiments. (*C*) Inhibition of FasL-induced cytolysis in Jurkat cells by the antagonistic peptides. Incorporation of [^{3}H]thymidine obtained with culture medium alone and with 30 ng/ml of FasL was used as reference for 100% and 0% survival, respectively. Survival (%) obtained over several doses of peptides is plotted. The results represent the arithmetic mean cpm of triplicate cultures.

Approximately 1,500 resonance units of FasL-Flag, Fas-Fc, TNF-α or TNFRI-Fc were immobilized on research-grade CM5 sensor chips (Biacore) by using standard *N*-ethyl-*N*-dimethylaminopropyl carbodiimide/*N*-hydroxysuccinimide coupling. Surface plasmon resonance measurements were carried out at a flow rate of 20 μl·min^{-1}. Data were analyzed with BIA EVALUATION 3.0 software (Biacore).

Cytotoxicity Assay. Twenty microliters of Jurkat cells at 1×10^5 cells/ml was plated in 96-well U-bottom plates. FasL-Flag (120 ng/ml in culture medium) was preincubated with an equal volume of peptide sample in PBS for 1 h at 37°C, and 20 μl of mixture was added to each well. After an incubation period of 24 h, each culture was pulsed with 1 μCi (1 Ci = 37 GBq) of thymidine for 24 h before harvesting on glass fiber filters. Incorporation of the radioactive label was measured by liquid scintillation counting (Wallac, Turku, Finland) and expressed as the arithmetic mean cpm of triplicate cultures.

Flow Cytometry Assay for Apoptosis. Apoptotic cells were detected by annexin V-FITC binding to phosphatidylserine expressed on the cell membrane in the early phase of apoptosis by using a commercial kit purchased from Roche as described by Vermes *et al.* (27). Briefly, 1×10^5 Jurkat cells were cultured with FasL-Flag (250 ng/ml) in the presence or absence of the peptide sample for 3 h. The cells were then washed and resuspended for 10 min in buffer containing calcium, FITC-conjugated annexin V, and propidium iodide (PI). Cells were analyzed by FACScan (Becton Dickinson). Early apoptotic cells were expressed as percentage of cells positive for annexin V and negative for PI.

Western Blotting. Downstream molecules involved in Fas signaling during apoptosis were examined. Jurkat cells (1×10^6/well) were cultured in six-well plates for 12 h, treated with or without 1 mM Kp7-6 for 2 h, and then treated with FasL at 100 ng/ml for indicated periods. Cells were then washed with chilled PBS and treated with lysis buffer. Cell lysates (15–30 μg) were separated by 12% SDS/PAGE, electroblotted onto nitrocellulose membranes (Osmonics, Westborough, MA), and probed with antiphospho-IκBα, anti-IκBα, antiphospho extracellular regulated kinase (ERK)1/2, anti-ERK2, and anti-β-actin Abs (Cell Signaling Technology, Beverly, MA). The membranes were then developed by using the enhanced chemiluminescence system(Amersham Pharmacia Biosciences).

Administration of Con A and Measurement of Serum Transaminase Activity. Hepatic damage was induced by injection of a single dose of 0.5 mg of Con A dissolved in pyrogen-free saline and administered to mice via the tail vein. Anti-FasL monoclonal antibody [MFL-4 (28)] or Fas mimetic peptide (Kp7-6 or Kp1-1) was diluted with pyrogen-free saline and injected in a single dose i.p. 30 min before Con A.

Blood samples were collected from mice at 12 h after Con A injection, and the serum was taken by centrifugation. Serum activities of alanine aminotransferase and aspartate aminotransferase were measured by Lippi–Guidi's method (Iatrozyme TA-LQ, Dia-Iatron, Tokyo) (29).

Statistical Analysis. Results are expressed as mean ± SE and analyzed by Student's *t* test or ANOVA where appropriate. Post hoc comparisons were performed by using the Scheffé test. A 95% confidence interval was used to define statistical significance.

Results

Molecular Model of Fas Receptor Complex. Fas, a member of the TNF superfamily, shares significant structural homology with the TNFR. The structure of the TNFR contains distinct "cystine-knot" repeating subdomains (30). Loop structures in the first three domains as well as β turns in proteins are considered to mediate roles in molecular recognition and binding (31). To develop a cystine-knot peptide mimetic, we identified critical sites of protein–protein interaction that might be disrupted or influenced by small molecules.

We developed a molecular model of the Fas and FasL complex (Fig. 1*A*) by using the crystal structure of the TNFR complex as well as other published models (23, 32). The overall features of the receptor–ligand interaction were noted to be very similar to that of the TNFR–ligand complex (22). Fas-FasL contact sites predicted by the molecular model are consistent with other mutation analysis

Table 1. Sequences of exocyclic peptidomimetics derived from Fas

Fas receptor	Exocyclic peptidomimetic	
Kp		
119 CNSTVC 124	Kp1-1	YCNSTVCY
Kp2		
77 DKAHFSSKC 85	Kp2-2	YCDKAEHFCY
Kp3		
103 CTRTQ 107	Kp3-2	YCNTRTQNTCY
Kp4		
69 CQEGKEY 75	Kp4-2	YCQEKEYCY
	Kp4-3	YCQERKEYCY
Kp7		
91 CDEGHGL 97	Kp7-2	YCDEGHLCY
	Kp7-3	YCDEGLCY
	Kp7-4	YCDEGYFCY
	Kp7-5	YCDEGEYCY
	Kp7-6	YCDEHFCY
	Kp7-7	YCDEHGLCY
	Kp7-8	YCDEHGQCY
	Kp7-9	YCDEKFCY
	Kp7-10	YCDEQFCY

Peptidomimetics were cyclized and constrained with cysteine disulfide bridges.

data (33). Our Fas-FasL structural model suggested five critical surfaces by which FasL can bind to its receptor compared to three sites identified in the TNFR (22). The amino acids in the loops Kp1-7 adopt well defined conformations (i.e., statistically allowed conformations) as judged by Ramachandran plots (34) and profile analyses (35).

Several peptide analogs were designed from the identified relevant loop structures. Each mimetic was optimized for its ability to mimic the binding conformation of the loop and for its ring size, which we have determined to be critical to reduce the inherent flexibility of mimetics. A set of mimetics that were selected for biological assay is shown in Table 1.

Inhibition of FasL Binding to the Receptor by Mimetics. The inhibition of FasL-Flag binding (100 ng/ml) to the Fas-Fc fusion protein immobilized onto plastic plates was then used to evaluate one aspect of mimetic activity. First-generation mimetics (Kp1-1, -2-2, -3-2, -4-2, and -7-2) were designed from different deduced binding sites of Fas to FasL and screened by using a binding inhibition assay (Fig. 1*B*). The results indicated that the Kp7 loop is a suitable surface for the design of mimetics as a template. We have reengineered and designed second and later generations of exocyclic peptides derived from the Kp7 loop surface. By analysis of the interaction site between FasL and Fas, the acidic residues (Asp and Glu) in the Kp7 loop appear to represent the most relevant residues involved in the interaction. Modification of other residues of Kp7 led to some improvement of inhibitory activities as seen with the Kp7 series (Fig. 1*B*).

Binding Affinity and Specificity of Mimetics. The Kp7 peptide analogs were expected to bind FasL and inhibit the interaction of FasL and Fas. To investigate the kinetics of binding of Kp7-6, the exocyclic species that mediated the best inhibitory activity to FasL, we performed surface plasmon resonance (BIAcore) analysis. FasL-Flag was immobilized onto a sensor chip and various concentrations of Kp7-6 were passed over the surface. The k_{on} and k_{off} rate constants were estimated to be 68.5 $M^{-1}s^{-1}$ and 7.65 $\times$ $10^{-4}s^{-1}$, respectively, and a K_d value of 11.2 μM was obtained from the ratio of the dissociation/association rate constants (Fig. 2*A*). Interestingly, Kp7-6 also bound to immobilized Fas (Fig. 2*B*). The k_{on} and k_{off} rate constants were estimated to be 24.1 $M^{-1}s^{-1}$ and 3.18 $\times$ $10^{-4}s^{-1}$, respectively, and the K_d of value 13.2 μM. Kp7-6 bound neither to the TNFR nor to TNF-α, suggesting that the mimetic is specific to FasL and interacts with the Fas receptor assembly.

Inhibition of FasL-Induced Cytotoxicity by Mimetics. To evaluate the effect of mimetics on Fas-mediated cytotoxicity, FasL-sensitive Jurkat cells were stimulated with the soluble FasL-Flag fusion protein in the presence or absence of various concentrations of mimetics. Generally, the inhibitory effects of mimetics on Fas-mediated cytotoxicity were consistent with the results of the FasL-binding inhibition (Fig. 1*B*). As shown in Fig. 3*A*, Kp7-6 showed a dose-dependent inhibitory activity, and at high doses, Kp7-6 protected >90% cells from Fas-mediated cytotoxicity. Kp7-10 also showed a dose-dependent inhibition (Fig. 1*C*). The cyclic peptides did not mediate any cytotoxicity for Jurkat cells in the range of concentration tested (data not shown). Neither Kp7-6 nor Kp7-10 used in combination with members of the Kp4 mimetics showed any significant synergy, suggesting that inhibition of the Kp7-binding site by itself is sufficient to antagonize FasL activity (data not shown).

Inhibition of FasL-Induced Apoptosis by Mimetics. To evaluate whether the designed mimetics can inhibit FasL-induced apoptosis, we analyzed phosphatidylserine (PS) externalization on the cell membrane by using annexin V. During the early apoptotic process, the cell membrane remains intact (as opposed to necrosis), and translocation of PS to the outer leaflet of the plasma membrane is a common feature of apoptosis that can be quantitatively measured using annexin V-FITC binding (27). Jurkat cells treated with FasL-Flag (200 ng/ml) for 3 h showed a marked increase in PS exposure compared with untreated cells (Fig. 3). The increase in Jurkat cell cytolysis was prevented by Kp7-6 in a dose-dependent

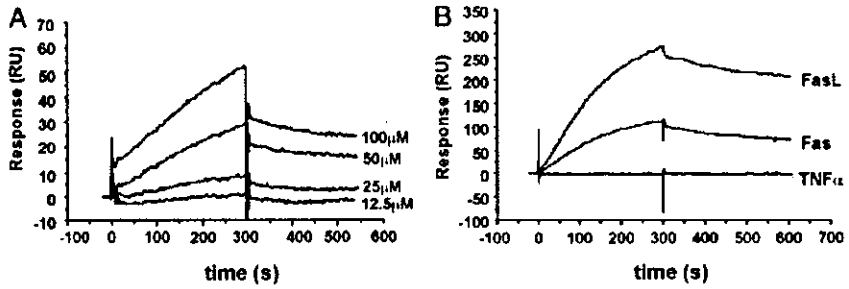

Fig. 2. Biosensor analysis of mimetic binding to immobilized FasL. The sensorgram shows the relative response in resonance units after background subtraction vs. time in seconds. The association phase injection time was 300 s followed by dissociation in buffer. (*A*) Sensorgrams showing the binding of Kp7-6 to FasL at Kp7-6 concentrations indicated in the graph. (*B*) Sensorgrams showing the interaction of Kp7-6 with Fas, FasL, and TNF-α.

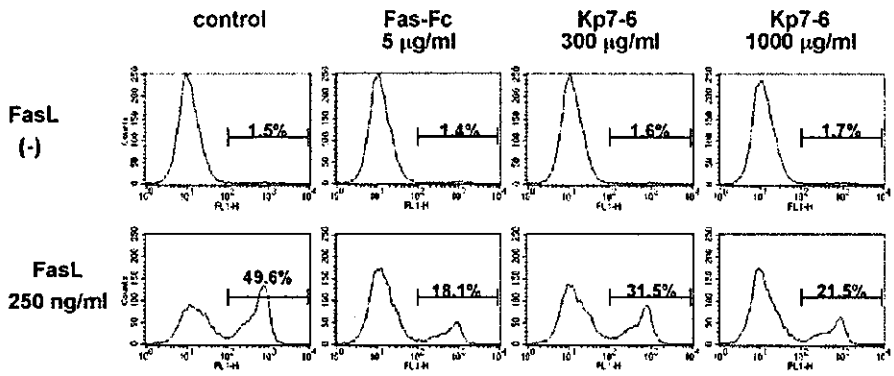

Fig. 3. Inhibition of FasL-induced apoptosis in Jurkat cells by the antagonistic peptide. Jurkat cells were treated with 250 ng/ml of FasL in the presence or absence of Kp7-6 for 3 h and stained with FITC-conjugated annexin V and propidium iodide. Ten thousand cells were analyzed in each condition. The number above each bar indicates the percentage of apoptotic (annexin-V$^+$) cells.

manner (Fig. 1*C*). These results show that Kp7-6 specifically protected FasL-induced cell lysis.

Modulation of NF-κB and ERK Activities by Mimetics. To evaluate how the designed mimetics alter FasL-mediated apoptosis, we analyzed IκBα, ERK, and c-jun N-terminal kinase (JNK) activation in Jurkat cells during the treatment of FasL. As shown in Fig. 4, Kp7-6 induced the phosphorylation of IκBα by 5 min in the presence of FasL. FasL alone did not activate IκBα significantly. These results indicate that Kp7-6 can cause activation of NF-κB, a constituent in a process that leads to inhibition of FasL-induced apoptosis. However, the IκBα effect was transient. We also noted that FasL leads to phosphorylation of ERK (by 5–30 min). ERK activation is thought to correlate with cell sensitivity to killing signals (36). We noted that ERK phosphorylation was significantly inhibited by Kp7-6, suggesting that the mimetic "desensitized" cells from death signals. These combined activities, namely phosphorylation of IκBα and reduction of ERK phosphorylation, are unexpected and represent a mechanistic approach to modulate apoptosis that follows receptor modulation.

The unexpected combination of enhanced survival signals (IκBα) and decreased apoptotic signals (inhibition of ERK phosphorylation) indicates that creating disabled receptor ensembles is a previously undescribed therapeutic approach. The JNK pathway was also examined, and no alteration in the activation signal either with or without pretreatment of Kp7-6 (data not shown) was seen,

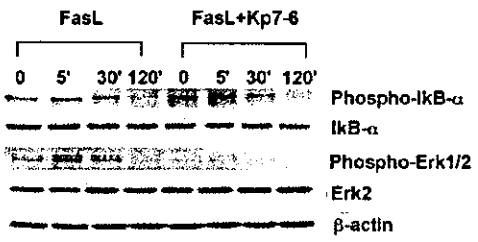

Fig. 4. Activation of the downstream NF-κB pathway and inhibition of mitogen-activated protein kinase kinase P42/44 in Jurkat cells by Kp7-6. Jurkat cells were pretreated with Kp7-6 for 2 h and then treated with 100 ng/ml of FasL at the indicated time course. The cells were lysed and analyzed by Western blotting. The expression of phospho-IκBα, IκBα, phospho-P42/44, and ERK-2 was analyzed. The expression of β-actin was analyzed as loading control. Kp7-6 at 1 mM clearly enhanced phosphorylation of IκBα in the presence of FasL at 5 min and significantly inhibited phosphorylation of Erk1/2 at 5–30 min, compared with the treatment of FasL alone.

indicating that JNK activation was not relevant for desensitization of cells.

Protection of Mice Against Con A-Induced Liver Injury by the Antagonistic Fas Mimetic Peptide. Next we investigated the *in vivo* effects of the mimetic, Kp7-6. FasL-induced apoptosis is one of the primary and dominant pathways by which liver cells undergo apoptosis under various conditions such as viral infection, drug toxicity, and other lesions (8, 15, 37). Several studies have found that blocking Fas signaling by either RNA interference or oligonucleotides limits the extent of liver damage (38, 39). We chose to investigate the antagonistic effect of Kp7-6 *in vivo* using the Con A-induced hepatitis model. C57BL/6 mice were pretreated i.p. with anti-FasL monoclonal antibody, Fas mimetic peptides, or saline. Thirty minutes later, animals were challenged i.v. with Con A or saline. The induction of liver damage and inflammatory hepatitis was evaluated by measuring the activities of two transaminases (alanine aminotransferase and aspartate aminotransferase) in the serum 12 h after Con A treatment. As shown in Fig. 5, the activities of both transaminase were reduced in Kp7-6-pretreated mice, indicating Kp7-6 blocked Fas-mediated hepatic injury *in vivo*. On the other hand, Kp1-1, a control mimetic, did not block hepatic injury

Discussion

Dysregulation of Fas has been implicated in several pathological conditions including cancer, autoimmunity, angiogenesis, and organ damage (19, 40). Fas has been shown to possess dual functions, namely modulation of apoptosis and proliferation (41). Thus, altering Fas regulation in a unilateral manner either by using genetic ablation or preventing FasL signals (by antibody or soluble receptors that exclude ligand binding to the receptor) may result in different outcomes than achieved by creating a dysfunctional Fas receptor complex. Here we have shown that rationally designed small molecules that form disabled receptor ensembles regulate Fas/FasL-mediated apoptotic function in a more novel manner than simply preventing ligand–receptor interactions.

A molecular model of Fas revealed that overall folding and interaction patterns with FasL are similar to those seen with the TNFR–TNF-β complex (32). In our earlier work, we found that the third domain of TNFR was critical for TNF-α to bind to its cognate receptor (22). Peptide mimetics derived from different regions of Fas indicated that the loop (Kp7) in the second domain was most critical (Fig. 1 *A* and *B*). Thus our results suggest that membrane proximal domains of TNF super family receptors may be critical for receptor–ligand stabilization and essential for signaling. This is also in agreement with our structural observations of the erbB receptor family (which are also type II receptors) where the membrane

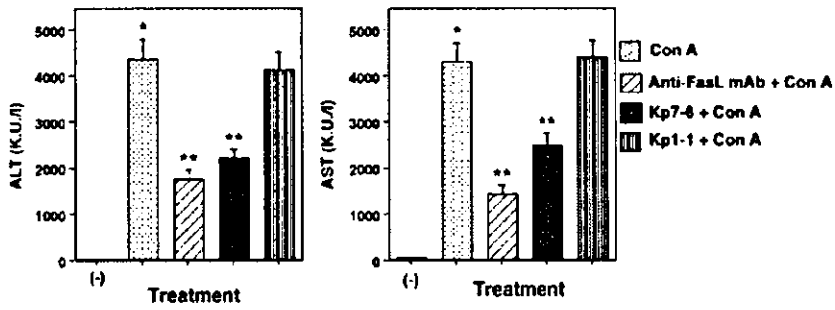

Fig. 5. Protection of mice against Con A-induced liver injury by the antagonistic Fas mimetic peptide. C57BL/6 mice were injected with 0.5 mg of Con A in saline or saline only as negative controls i.v. Anti-FasL monoclonal antibody (MFL-4, 0.5 mg/mouse) or Fas mimetic peptide (Kp7-6 or Kp1-1, 3 mg per mouse) in saline was injected i.p. 30 min before Con A. Blood samples were obtained 12 h after Con A injection, and serum alanine aminotransferase and aspartate aminotransferase levels were measured. *, $P < 0.0001$ vs. control; **, $P < 0.01$ vs. Con A-treated mice.

proximal domain, which shares structural homology to the TNFR, is critical for signaling (42). Thus, we propose that an antibody or small molecule that binds to membrane proximal domains will have more pronounced effects on signaling aspects of the receptor system.

The K_d of the Kp7-6–FasL interaction was of less affinity than that noted for Fas–FasL interactions (43). Although Kp7-6 is a weak binding species, it is able to alter Fas functions *in vitro* and *in vivo*. The dissociation rate (k_{off}) of Kp7-6 was similar to an antigen–antibody interaction, which suggests that Kp7-6 forms a stable receptor complex (26). The k_{off} value is considered a critical indicator in the development of therapeutics with biological activity (44, 45) and generally correlates with potent biological effects (46). These observations help explain the observed biological activity of Kp7-6.

Kp7-6 is selective to the Fas receptor complex. Selectivity of small molecules binding to large receptor complexes is difficult to achieve due to the limited surface area available for the small molecule to interact with its receptor. Selectivity is notable for Kp7-6, because several members of the superfamily share significant homology. To assess the specificity of this interaction, Fas, FasL, and TNF-α were immobilized onto a sensor chip. Kp7-6 bound to FasL but not to TNF-α, which indicates Kp7-6 binds to FasL specifically (Fig. 2*B*). On the other hand, Kp7-6 bound not only to FasL but also to Fas (Fig. 2*B*), yet Kp7-6 did not bind to the closely related TNFRs. These observations are reminiscent of features of the soluble TNFR1 (p55), which has been shown to form antiparallel homodimeric complexes in the absence of ligand (30). Our results in this study suggest that soluble Fas may also form such antiparallel dimers, and the Kp7 loop may be involved in dimer formation. Thus these results suggest that Kp7-6 is selective to Fas and may function like a minisoluble Fas receptor.

Small molecules such as Kp7-6 may disable Fas by a different mechanism from the macromolecular anti-Fas antibodies. Unlike anti-Fas macromolecular species that have been shown to limit Con A-induced hepatitis, Kp7-6 is a small molecule, not large enough to preclude the interaction of FasL with Fas. This raises the possibility that Kp7-6 acts by promoting a defective signaling complex. The Kp7-6 mimetic, described above, is derived from the Fas receptor and has the propensity to bind to both the receptor and its ligand with comparable affinity. This suggests that Kp7-6 could either bind to Fas and prevent FasL from forming a stable complex with the receptor or bind to both FasL and Fas and form a defective signaling complex. A proposed scheme is shown in Fig. 6.

Furthermore, Fas/FasL-induced apoptosis follows two major pathways: (*i*) an intrinsic pathway, often referred to as a caspase-dependent mitochondrial pathway (47, 48); and (*ii*) an extrinsic pathway that is caspase independent and involves NF-κB and JNK (40). A secondary signaling process, the ERK pathway, has been shown to be proapoptotic or to act as an attenuator of apoptosis (36, 49). Our studies revealed that the FasL–Kp7-6 complex weakly stimulated NF-κB but suppressed ERK activation. Kp7-6 had no effect on the JNK activation state. Activation of NF-κB is closely linked to regulation of antiapoptotic molecules (41, 50, 51). Thus,

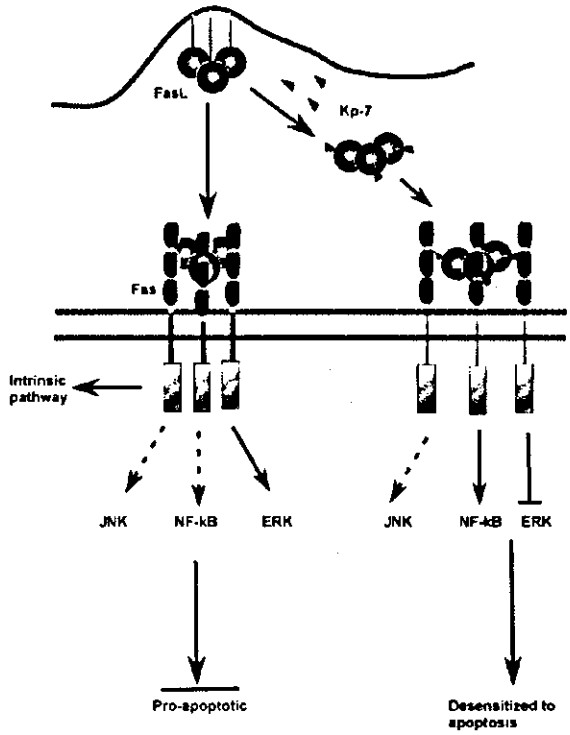

Fig. 6. Proposed mechanism by which Kp7-6 desensitize Fas/FasL proapoptotis signals. Fas-FasL-mediated apoptosis follows two major pathways : (*i*) intrinsic and (*ii*) extrinsic. Key apoptotic signal regulators (NF-κB, JNK, and ERK) in the pathways (*Left*) and the signal modification obtained by Kp7-6 (*Right*) are shown. Kp7-6 binding to either FasL or Fas or both creates a defective receptor complex ensemble. As a consequence, NF-κB is activated, but ERK activation is inhibited. The combined modulation of these two key regulator leads to "desensitization" of cells to apoptosis. The JNK pathway remains unaltered.

weak activation of NF-κB is consistent with the antiapoptotic events observed. In several studies, activation of JNK has been shown to be not relevant for apoptotic signals (49, 52), and indeed JNK activation was unaltered by the FasL–Kp7-6 complex, indicating that JNK may play an insignificant role in Fas-mediated signals in this system.

The FasL–Kp7-6 complex inhibited ERK activation. In general, activation of ERK is considered an indicator of cell proliferation (53–55). However, under some circumstances, depending on the cell type and the level of Fas expression, activation of ERK plays a secondary role: to sensitize cells to FasL-induced apoptosis (36, 49, 56). Thus, in the context of Fas/FasL receptor signaling, disabling ERK by the FasL–Kp7-6 complex may be considered a "FasL desensitization" stimulus. Kp7-6 thus desensitizes or attenuates FasL-mediated apoptosis. By creating a defective complex, Kp7-6 protects cells from FasL-induced apoptosis by a complex pattern of signals, the concurrence of which has not been greatly appreciated.

The specific mechanism by which apoptotic receptors such as Fas and TNFR1 (p55) mediate Con A-induced hepatitis is not fully understood. Genetic studies using Fas-deficient *lpr/lpr* mice indicate mechanisms other than that mediated by the Fas-FasL system also involved in this process (12, 16). Nevertheless, inhibition of Fas has some beneficial effect in limiting liver damage. Thus, Fas is a primary drug target against liver injury, and several approaches have been reported including gene therapy (57), interference RNA (39), and monoclonal antibody (11). Kp7-6 represents a previously unreported small molecule that can effectively disable Fas receptor function *in vitro* and that limits liver injury *in vivo* comparable to the effects of the anti-Fas monoclonal antibody.

Kp7-6 is a rationally fashioned peptide mimetic that demonstrates specific anti-FasL activity *in vitro* and *in vivo*. Signaling studies show that Kp7-6 is able to protect cells from Fas-mediated apoptosis by promoting NF-κB activity and by inhibiting ERK activity. Our work suggests that small molecular drugs can be developed to modulate cell surface receptors using a novel approach that in essence creates spacers between functional receptor proteins and creates dysfunctional receptor complexes. We believe the development of small molecules that are specific for other members of the TNFR family may represent a general way of studying functional aspects of receptor subdomains that will facilitate the rational development of therapeutics.

We thank the Biosensor/Interaction Analysis and Structural Biology Core Group, Department of Medicine, University of Pennsylvania, for assistance with Biacore binding studies and the Protein Chemistry Laboratory, University of Pennsylvania, for peptide synthesis and purification. This work was supported by the Abramson Family Cancer Research Institute and by grants from the National Institutes of Health, the National Cancer Institute, the National Institute of Neurological Disorders and Stroke, and the Cancer Center, University of Pennsylvania.

1. Nagata, S. & Golstein, P. (1995) *Science* **267**, 1449–1456.
2. Watanabe-Fukunaga, R., Brannan, C. I., Itoh, N., Yonehara, S., Copeland, N. G., Jenkins, N. A. & Nagata, S. (1992) *J. Immunol.* **148**, 1274–1279.
3. Suda, T., Takahashi, T., Golstein, P. & Nagata, S. (1993) *Cell* **75**, 1169–1178.
4. Kayagaki, N., Kawasaki, A., Ebata, T., Ohmoto, H., Ikeda, S., Inoue, S., Yoshino, K., Okumura, K. & Yagita, H. (1995) *J. Exp. Med.* **182**, 1777–1783.
5. Mariani, S. M., Matiba, B., Baumler, C. & Krammer, P. H. (1995) *Eur. J. Immunol.* **25**, 2303–2307.
6. Biancone, L., Martino, A. D., Orlandi, V., Conaldi, P. G., Toniolo, A. & Camussi, G. (1997) *J. Exp. Med.* **186**, 147–152.
7. Krammer, P. H. (1999) *Adv. Immunol.* **71**, 163–210.
8. Famularo, G., Nucera, E., Marcellini, S. & De Simone, C. (1999) *Med. Hypotheses* **53**, 50–62.
9. Tiegs, G., Hentschel, J. & Wendel, A. (1992) *J. Clin. Invest.* **90**, 196–203.
10. Mizuhara, H., O'Neill, E., Seki, N., Ogawa, T., Kusunoki, C., Otsuka, K., Satoh, S., Niwa, M., Senoh, H. & Fujiwara, H. (1994) *J. Exp. Med.* **179**, 1529–1537.
11. Seino, K., Kayagaki, N., Takeda, K., Fukao, K., Okumura, K. & Yagita, H. (1997) *Gastroenterology* **113**, 1315–1322.
12. Tagawa, Y., Sekikawa, K. & Iwakura, Y. (1997) *J. Immunol.* **159**, 1418–1428.
13. Tagawa, Y., Kakuta, S. & Iwakura, Y. (1998) *Eur. J. Immunol.* **28**, 4105–4113.
14. Watanabe, Y., Morita, M. & Akaike, T. (1996) *Hepatology* **24**, 702–710.
15. Gantner, F., Leist, M., Lohse, A. W., Germann, P. G. & Tiegs, G. (1995) *Hepatology* **21**, 190–198.
16. Toyabe, S., Seki, S., Iiai, T., Takeda, K., Shirai, K., Watanabe, H., Hiraide, H., Uchiyama, M. & Abo, T. (1997) *J. Immunol.* **159**, 1537–1542.
17. Kusters, S., Tiegs, G., Alexopoulou, L., Pasparakis, M., Douni, E., Kunstle, G., Bluethmann, H., Wendel, A., Pfizenmaier, K., Kollias, G., *et al.* (1997) *Eur. J. Immunol.* **27**, 2870–2875.
18. Ksontini, R., Colagiovanni, D. B., Josephs, M. D., Edwards, C. K., III, Tannahill, C. L., Solorzano, C. C., Norman, J., Denham, W., Clare-Salzler, M., MacKay, S. L., *et al.* (1998) *J. Immunol.* **160**, 4082–4089.
19. Maggi, C. A. (1998) *Pharmacol. Res.* **38**, 1–34.
20. Okuda, Y., Sakoda, S., Fujimura, H., Nagata, S., Yanagihara, T. & Bernard, C. C. (2000) *Biochem. Biophys. Res. Commun.* **275**, 164–168.
21. Park, B. W., Zhang, H. T., Wu, C., Berezov, A., Zhang, X., Dua, R., Wang, Q., Kao, G., O'Rourke, D. M., Greene, M. I. & Murali, R. (2000) *Nat. Biotechnol.* **18**, 194–198.
22. Takasaki, W., Kajino, Y., Kajino, K., Murali, R. & Greene, M. I. (1997) *Nat. Biotechnol.* **15**, 1266–1270.
23. Bajorath, J. (1999) *J. Comput. Aided Mol. Des.* **13**, 409–418.
24. Cheng, X., Kinosaki, M., Takami, M., Choi, Y., Zhang, H. & Murali, R. (2004) *J. Biol. Chem.* **279**, 8269–8277.
25. Schneider, P., Bodmer, J. L., Holler, N., Mattmann, C., Scuderi, P., Terskikh, A., Peitsch, M. C. & Tschopp, J. (1997) *J. Biol. Chem.* **272**, 18827–18833.
26. Berezov, A., Zhang, H. T., Greene, M. I. & Murali, R. (2001) *J. Med. Chem.* **44**, 2565–2574.
27. Vermes, I., Haanen, C., Steffens-Nakken, H. & Reutelingsperger, C. (1995) *J. Immunol. Methods* **184**, 39–51.
28. Kayagaki, N., Yamaguchi, N., Nagao, F., Matsuo, S., Maeda, H., Okumura, K. & Yagita, H. (1997) *Proc. Natl. Acad. Sci. USA* **94**, 3914–3919.
29. Lippi, U. & Guidi, G. (1970) *Clin. Chim. Acta* **28**, 431–437.
30. Naismith, J. H., Devine, T. Q., Kohno, T. & Sprang, S. R. (1996) *Structure (Cambridge, U.K.)* **4**, 1251–1262.
31. Leszczynski, J. F. & Rose, G. D. (1986) *Science* **234**, 849–855.
32. Banner, D. W., D'Arcy, A., Janes, W., Gentz, R., Schoenfeld, H. J., Broger, C., Loetscher, H. & Lesslauer, W. (1993) *Cell* **73**, 431–445.
33. Beltinger, C., Bohler, T., Karawajew, L., Ludwig, W. D., Schrappe, M. & Debatin, K. M. (1998) *Br. J. Haematol.* **102**, 722–728.
34. Ramachandran, G. N. & Venkatachalam, C. M. (1968) *Biopolymers* **6**, 1255–1262.
35. Zhang, K. Y. & Eisenberg, D. (1994) *Protein Sci.* **3**, 687–695.
36. Tran, S. E., Holmstrom, T. H., Ahonen, M., Kahari, V. M. & Eriksson, J. E. (2001) *J. Biol. Chem.* **276**, 16484–16490.
37. Kakinuma, C., Takagaki, K., Yatomi, T., Nakamura, N., Nagata, S., Uemura, A. & Shibutani, Y. (1999) *Toxicol. Pathol.* **27**, 412–420.
38. Zhang, H., Cook, J., Nickel, J., Yu, R., Stecker, K., Myers, K. & Dean, N. M. (2000) *Nat. Biotechnol.* **18**, 862–867.
39. Song, E., Lee, S. K., Wang, J., Ince, N., Ouyang, N., Min, J., Chen, J., Shankar, P. & Lieberman, J. (2003) *Nat. Med.* **9**, 347–351.
40. Sharma, K., Wang, R. X., Zhang, L. Y., Yin, D. L., Luo, X. Y., Solomon, J. C., Jiang, R. F., Markos, K., Davidson, W., Scott, D. W. & Shi, Y. F. (2000) *Pharmacol. Ther.* **88**, 333–347.
41. Wajant, H., Pfizenmaier, K. & Scheurich, P. (2003) *Cytokine Growth Factor Rev.* **14**, 53–66.
42. Berezov, A., Chen, J., Liu, Q., Zhang, H. T., Greene, M. I. & Murali, R. (2002) *J. Biol. Chem.* **277**, 28330–28339.
43. Starling, G. C., Bajorath, J., Emswiler, J., Ledbetter, J. A., Aruffo, A. & Kiener, P. A. (1997) *J. Exp. Med.* **185**, 1487–1492.
44. Benveniste, M. & Mayer, M. L. (1991) *Br. J. Pharmacol.* **104**, 207–221.
45. Yiallouros, I., Vassiliou, S., Yiotakis, A., Zwilling, R., Stocker, W. & Dive, V. (1998) *Biochem. J.* **331**, 375–379.
46. Moosmayer, D., Wajant, H., Gerlach, E., Schmidt, M., Brocks, B. & Pfizenmaier, K. (1996) *J. Interferon Cytokine Res.* **16**, 471–477.
47. Waring, P. & Mullbacher, A. (1999) *Immunol. Cell Biol.* **77**, 312–317.
48. Yin, X. M. & Ding, W. X. (2003) *Curr. Mol. Med.* **3**, 491–508.
49. Wilson, D. J., Alessandrini, A. & Budd, R. C. (1999) *Cell Immunol.* **194**, 67–77.
50. Mandal, M., Maggirwar, S. B., Sharma, N., Kaufmann, S. H., Sun, S. C. & Kumar, R. (1996) *J. Biol. Chem.* **271**, 30354–30359.
51. Wajant, H., Haas, E., Schwenzer, R., Muhlenbeck, F., Kreuz, S., Schubert, G., Grell, M., Smith, C. & Scheurich, P. (2000) *J. Biol. Chem.* **275**, 24357–24366.
52. Low, W., Smith, A., Ashworth, A. & Collins, M. (1999) *Oncogene* **18**, 3737–3741.
53. Cobb, M. H., Hepler, J. E., Cheng, M. & Robbins, D. (1994) *Semin. Cancer Biol.* **5**, 261–268.
54. Marais, R. & Marshall, C. J. (1996) *Cancer Surv.* **27**, 101–125.
55. Fan, M. & Chambers, T. C. (2001) *Drug Resist. Updat.* **4**, 253–267.
56. Engedal, N. & Blomhoff, H. K. (2003) *J. Biol. Chem.* **278**, 10934–10941.
57. Fujino, M., Kawasaki, M., Funeshima, N., Kitazawa, Y., Kosuga, M., Okabe, K., Hashimoto, M., Yaginuma, H., Mikoshiba, K., Okuyama, T., *et al.* (2003) *Gene Ther.* **10**, 1781–1790.

International Immunology, Vol. 16, No. 2, pp. 215–222
doi: 10.1093/intimm/dxh020

Impaired IFN-γ production of V_α24 NKT cells in non-remitting sarcoidosis

Seiichiro Kobayashi[1], Yoshikatsu Kaneko[1], Ken-ichiro Seino[4,5], Yoshihito Yamada[2], Shinichiro Motohashi[1], Junzo Koike[1], Kaoru Sugaya[1], Takayuki Kuriyama[2], Shigetaka Asano[6], Tomiyasu Tsuda[7], Hiroshi Wakao[4], Michishige Harada[4], Satoshi Kojo[4], Toshinori Nakayama[1,3] and Masaru Taniguchi[1,4]

Departments of [1]Molecular Immunology, [2]Respirology and [3]Medical Immunology, Graduate School of Medicine, Chiba University, Chiba 260-8670, Japan
[4]Laboratory for Immune Regulation, RIKEN Research Center for Allergy and Immunology, Yokohama 230-0045, Japan
[5]PRESTO, Japan Science and Technology Corp., Saitama 332-0012, Japan
[6]Division of Molecular Therapy, Institute of Medical Science, University of Tokyo, Tokyo 113-0033, Japan
[7]Third Department of Internal Medicine, Oita Medical University, Oita 879-5593, Japan

Keywords: cytokine, human, inflammation, lung, T_h1/T_h2 cell

Abstract

Sarcoidosis is a systemic disorder associated with granuloma characterized by an abnormal T_h1-type cytokine production and accumulation of T_h1 CD4 T cells in the granuloma lesions, suggesting an importance of T_h1 responses in sarcoidosis. However, the pathogenesis of sarcoidosis remains to be solved. Here, we investigated the nature of V_α24 NKT cells with immunoregulatory functions in sarcoidosis. Patients with non-remitting sarcoidosis displayed a decrease in the number of V_α24 NKT cells in peripheral blood, but an accumulation of these cells in granulomatous lesions. When stimulated with the specific glycolipid ligand, α-galactosylceramide, peripheral blood V_α24 NKT cells from patients with non-remitting disease produced significantly less IFN-γ than those from healthy volunteers, but normal levels of IL-4. The reduced IFN-γ production was observed only in V_α24 NKT cells and not conventional CD4 T cells, but was normal in patients with remitting disease, suggesting that non-remitting sarcoidosis involves an insufficient IFN-γ production of V_α24 NKT cells which is well correlated with disease activity. Thus, these results suggest that V_α24 NKT cells play a crucial role in the disease status of sarcoidosis.

Introduction

NKT cells constitute a unique lymphocyte subpopulation characterized by expression of NK cell markers, and an invariant antigen receptor encoded by V_α14 and J_α281 gene segments in mice (1) and V_α24 and J_αQ gene segments in humans (2,3). Activated V_α14 NKT and V_α24 NKT cells produce both IFN-γ and IL-4 (4–6), for which an imbalance has previously been found to be associated with disease. V_α14 NKT cells exert regulatory activity which protects against development of autoimmune diseases such as Type 1 diabetes in NOD mice (7,8) and maintains transplantation tolerance (9,10). V_α14 NKT cells have also been reported to protect against microbial infections and subsequent host responses as in the granuloma formation of *Mycobacterium tuberculosis* infection (11).

Sarcoidosis is a systemic disorder characterized by its pathological hallmark, the non-caseating granuloma (12). Its presentation varies from an asymptomatic stage with abnormal findings on chest radiography to a progressive stage with multi-organ failure; the illness appears as both a self-limiting and a chronic progressive form, the latter showing episodic recrudescence and remission. Although the precise pathogenesis of sarcoidosis remains unclear, it is thought to involve an exaggerated cellular immune response against unknown antigens leading to granuloma formation in genetically pre-

The first two authors contributed equally to this work

Correspondence to: M. Taniguchi; E-mail: taniguti@med.m.chiba-u.ac.jp

Transmitting editor: M. Miyasaka

Received 29 August 2003, *accepted* 17 October 2003

Table 1. Characteristics of the sarcoidosis patients and normal controls

	Remitting	Non-remitting	Normal controls
Total number	30	13	22
Age (mean ± SD)	36.8 ± 8.9	41.2 ± 12.2	32.5 ± 7.5
Gender			
male	17	6	16
female	13	7	6
Stage of disease			
I	13	4	-
II	16	7	-
III	1	2	-

diseased hosts (13). Several reports have indicated elevated levels of T_h1-type cytokines, such as IFN-γ, in bronchoalveolar lavage fluid (BALF) of sarcoidosis patients (14) and an accumulation of T_h1 CD4 T cells in the granuloma lesions (15,16), suggesting an importance of T_h1 response in the pathogenesis of sarcoidosis and the elimination of unknown sarcoidosis pathogens.

In this report, we examined the function of $V_\alpha24$ NKT cells in patients with remitting and non-remitting sarcoidosis. We used mouse $V_\alpha14$ NKT cells instead of relying on limited numbers of human $V_\alpha24$ NKT cells to measure antigen-presenting ability and performed single-cell RT-PCR to detect cytokine production. The results suggest that, in contrast to previous reports, decreased numbers of $V_\alpha24$ NKT cells and their abnormally low production of IFN-γ are well associated with disease status in sarcoidosis.

Methods

Study population and ethical considerations

The diagnoses of pulmonary sarcoidosis were established in all patients based on clinical criteria with confirmation of non-caseating granulomas on tissue biopsies (17). The characteristics of the sarcoidosis patients and normal controls are shown in Table 1. These patients had no histories of using steroids or other anti-inflammatory drugs at the time of sampling. Staging of sarcoidosis was defined as the criteria determined in the Consensus Conference (18). The classification of patients was defined as follows. Remitting patients: abnormal findings on chest radiography have disappeared, improved or are stable over ~3 months of observation. Non-remitting patients: abnormal findings fluctuate or worsen. The disease status in individual patients was defined as follows. Stable status: abnormal findings on chest radiography have disappeared, improved or are stable over ~3 months of observation. Active status: abnormal findings fluctuate or worsen. Some muscular sarcoidosis patients were also examined for detecting NKT cell accumulation in the lesions (Fig. 5). All subjects gave consent after being informed about the nature and purpose of the study. Local ethics committee approval was obtained.

Cell preparation

Peripheral blood and BALF samples were collected from each patient on the same day and within 6 months of disease onset, and mononuclear cells prepared as described (19).

Flow cytometric analysis

Mononuclear cells were stained with FITC-conjugated anti-TCR $V_\alpha24$ mAb (C15; Coulter-Immunotech, Miami, FL), phycoerythrin (PE)-conjugated anti-TCR $V_\beta11$ mAb (C21; Coulter-Immunotech) and CyChrome-conjugated anti-CD3 mAb (UCTH1; PharMingen, San Diego, CA) as described previously (19). For intracellular staining, non-adherent peripheral blood mononuclear cells (PBMC) were stimulated with 12-phorbol 13-myristate acetate (PMA) and ionomycin for 4 h as described (20). Then, the cells were permeabilized and stained with CyChrome-conjugated anti-CD4 mAb (RPA-T4), FITC-conjugated anti-IFN-γ (4S.B3) and PE-conjugated anti-IL-4 mAb (8D4-8) (all from PharMingen). Lymphocytes were gated by forward and side scatter. Live lymphocytes were analyzed on an Epics-XL-MCL (Beckman Coulter, Hialeah, FL).

Evaluation of α-galactosylceramide (α-GalCer)-presenting ability of antigen-presenting cell (APC)

MACS-enriched $CD3^-$ human PBMC were incubated with α-GalCer (100 ng/ml; Kirin Brewery, Gunma, Japan) or its vehicle as described previously (19) and used as APC. Irradiated α-GalCer-pulsed APC (5×10^5) were co-cultured with 2×10^5 spleen cells from RAG KO/$V_\alpha14$Tg$V_\beta8$Tg mice (21) for 60 h. The proliferative responses of the mouse $V_\alpha14$ NKT cells were evaluated by thymidine incorporation in the last 12 h. The stimulation index was calculated from the following formula: (c.p.m. of the α-GalCer-treated group)/(c.p.m. of the vehicle-treated group).

Detection of $V_\alpha24$ TCR and IFN-γ mRNA by single-cell RT-PCR

The detection of $V_\alpha24$ and IFN-γ transcripts in the plate-bound anti-CD3-stimulated and sorted $V_\alpha24^+V_\beta11^+$ cells was performed with single-cell RT-PCR as previously described (22). PCR primer pairs used were as follows: TCR $V_\alpha24$ (5′-CAAAGTCGAACGGAAGATATAC-3′) and TCR C_α (5′-CCTCATGTCTAGCACAGTTTT-3′), and IFN-γ (5′-GAGCCAAATTGTCTCCTTTTACTT-3′, 5′-GTAGGCAGGACAACCATTACTGGG-3′). PCR was carried out at 94°C for 30 s, 55°C for 30 s and 72°C for 1 min for 40 cycles for TCR $V_\alpha24$, IFN-γ and IL-4, or 25 cycles for GAPDH on a Takara PCR Thermal Cycler SP (Takara Shuzo, Shiga, Japan). An aliquot (1 μl) of the first-round PCR product was used for the second-round PCR with following primers: TCR $V_\alpha24$ (5′-ATGCAGACACAAAGCAAAGCAAAGCTC-3′) and TCR C_α (5′-GGCAGACAGACTTGTCACTGGA-3′), and IFN-γ (5′-ATGACCAGAGCATCCAAAAGAGTG-3′, 5′-CGCTTCCCTGTTTTAGCTGCTGGC-3′).

Quantification of IFN-γ and IL-4 produced by $V_\alpha24$ NKT cells.

The transcriptional levels of IFN-γ, IL-4 and GAPDH of cultured $V_\alpha24^+V_\beta11^+$ NKT cells were assessed by semi-quantitative RT-PCR. PBMC were cultured with recombinant human IL-2 (50 U/

ml, Immunace; Shionogi, Osaka, Japan) and α-GalCer (10 ng/ml) for 7 days. $V_\alpha24^+V_\beta11^+$ double-positive cells were sorted on a FACS Vantage. Cells (10^3) were suspended in 200 μl of complete medium in a 96-well round-bottom plate and stimulated with PMA (10 ng/ml; Sigma, St Louis, MO) and ionomycin (1 μM; Calbiochem, San Diego, CA) for 4 h. RNA extraction and reverse transcription were performed as described previously (23). cDNA samples was subjected to PCR using the following primers: IFN-γ, 5′-AGTTATATC-TTGGCTTTTCA-3′, 5′-ACCGAATAATTAGTCAGCTT-3′; IL-4, 5′-CTTCCCCCTCTGTTCTTCCT-3′, 5′-TTCCTGTCGAGCCGT-TTCAG-3′; or GAPDH, 5′-CCATGGGGAAGGTGAAGGT-3′, 5′-ATGACCCTTTTGGCTCCCC-3′. A 30-cycle reaction was performed for IFN-γ and IL-4, and a 25-cycle reaction for GAPDH. For obtaining standardization curves, cDNAs of serial 3-fold dilutions (corresponding to 1.4~9000 copies of cDNA) were subjected to PCR with primers listed above. PCR products were hybridized with a [^{32}P]dCTP-labeled probe and the intensity of each band quantified by densitometry (Fujix BAS2500; Fujifilm I&I, Tokyo, Japan). Copy numbers of IFN-γ, IL-4 and GAPDH in each sample were estimated with the standard curves.

Analysis of $V_\alpha24$ NKT cells in granuloma lesions

RNA extraction was performed with anterior scalene muscle lymph nodes of seven pulmonary sarcoidosis patients, hilar lymph nodes of four lung cancer patients, skeletal muscle of five muscular sarcoidosis and PBMC from three normal controls. RNA extracted from the skeletal muscle of normal controls was purchased from Clontech (K4008-1; Palo Alto, CA). Synthesized cDNA samples were subjected to PCR with following primers: TCR $V_\alpha24$–J_αQ, 5′-GGGAGAGGTCCTG-TTTCC-3′, 5′-CCTCTTCCAAAGTATAGCCTCCCCAG-3′; TCR C_α, 5′-GAACCCTGACCCTGCCGTGTA-3′, 5′-CACTTTCAGG-AGGAGGATTCG -3′. The primer pairs for IFN-γ and IL-4 are described above. A 30-cycle reaction was performed for TCR $V_\alpha24$–J_αQ and a 20-cycle reaction for TCR C_α. Quantification of gene transcripts was performed as described above.

Statistical analysis

All data were expressed as the mean ± SD. Statistical analyses were performed using Student's *t*-test. $P < 0.05$ was considered as statistically significant.

Results

Decreased IFN-γ production of $V_\alpha24$ NKT cells in non-remitting, but not remitting, sarcoidosis

$V_\alpha24$ NKT cells are known to produce abundant cytokines that regulate various immune responses. We therefore looked for functional defects in cytokine production of $V_\alpha24$ NKT cells in

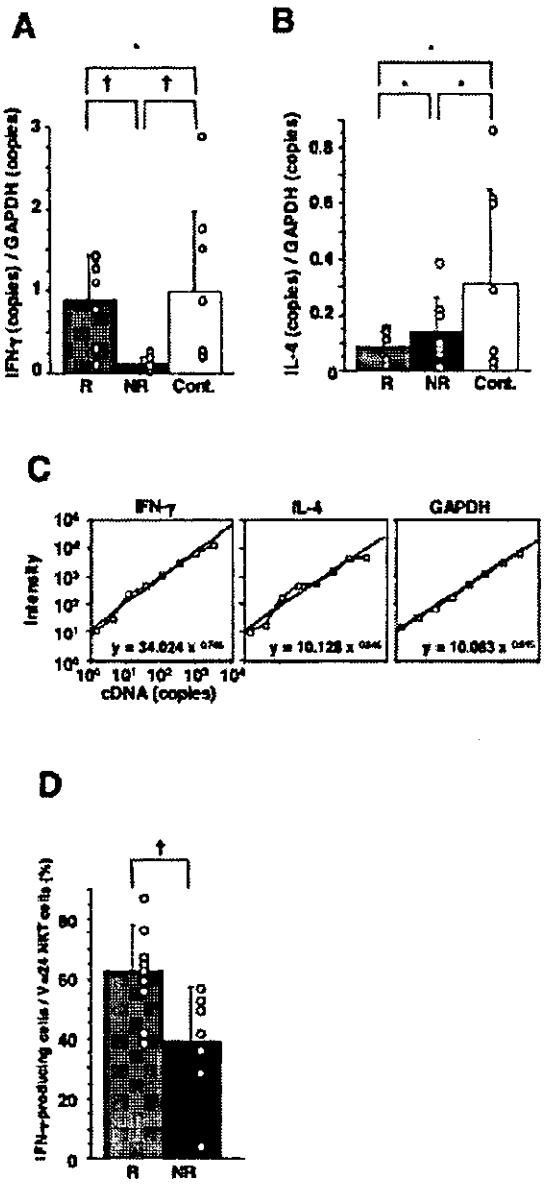

Fig. 1. Decreased IFN-γ production of $V_\alpha24$ NKT cells in non-remitting sarcoidosis. (A and B) The levels of IFN-γ (A) and IL-4 (B) transcripts in $V_\alpha24$ NKT cells induced by PMA and ionomycin were examined by semi-quantitative RT-PCR analysis. The copy numbers for IFN-γ and IL-4 were estimated using standard curves generated in each assay and normalized with copy numbers of GAPDH. Mean values of remitting (R, $n = 7$) and non-remitting (NR, $n = 8$) sarcoidosis patients and normal controls (Cont., $n = 8$) are shown with SD; $^\dagger P < 0.05$, *differences are not significant. (C) Representative standard curves generated for IFN-γ, IL-4 and GAPDH. Serial dilutions of the standard DNA template were amplified and hybridized with a specific [^{32}P]dCTP probe. Radioactivity was expressed as intensity and plotted against template concentrations. (D) The IFN-γ-producing potential of freshly prepared $V_\alpha24$ NKT cells upon CD3-stimulation for 6 h. Freshly prepared PBMC were stimulated with immobilized anti-CD3 mAb and $V_\alpha24^+V_\beta11^+$ double-positive cells sorted in a 96-well plate at a single cell per well. $V_\alpha24$ TCR and IFN-γ mRNA were detected by single-cell RT-PCR. Mean values of the percentages of IFN-γ-producing cells in remitting (R, $n = 9$) and non-remitting sarcoidosis patients (NR, $n = 7$) are shown with SD; $^\dagger P < 0.05$.

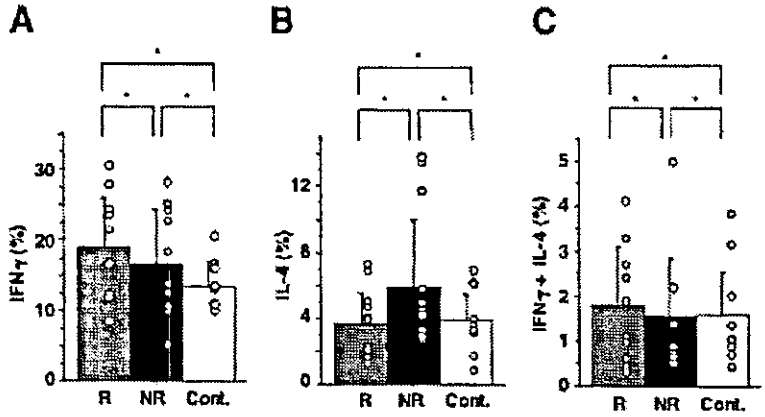

Fig. 2. Normal production of IFN-γ and IL-4 in CD4 T cells from sarcoidosis patients. Non-adherent PBMC were stimulated with PMA and ionomycin for 4 h, and intracellular cytokine staining (IFN-γ/IL-4) carried out using anti-CD4 staining. The percentages of IFN-γ+ (A), IL-4- (B) and (IFN-γ + IL-4)-producing (C) CD4 T cells in remitting (R, n = 10) and non-remitting (NR, n = 11) sarcoidosis patients and normal controls (Cont., n = 10) were determined. Mean values with SD are shown; *differences are not significant.

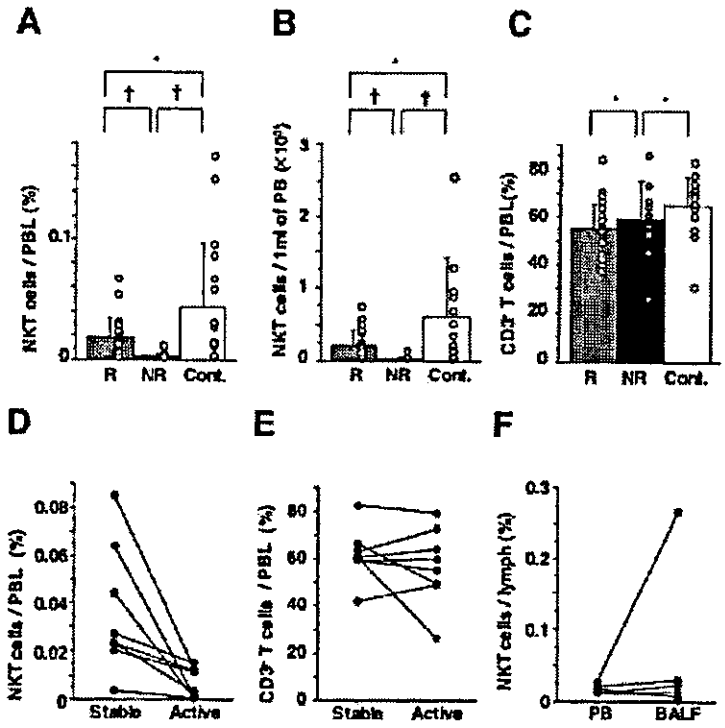

Fig. 3. Frequency of $V_\alpha24$ NKT cells in the peripheral blood of sarcoidosis patients. (A–C) Percentages of $V_\alpha24^+V_\beta11^+$ NKT cells in peripheral blood lymphocytes (PBL) (A), the absolute numbers of $V_\alpha24^+V_\beta11^+$ NKT cells per 1 ml of PBMC (B) and percentages of $CD3^+$ T cells in PBMC (C) from remitting (R, n = 20) and non-remitting (NR, n = 10) sarcoidosis patients and normal controls (Cont., n = 17) were assessed, and mean values with SD are shown; †$P < 0.05$, *differences are not significant. (D and E) Percentages of $V_\alpha24^+V_\beta11^+$ NKT cells (D) and $CD3^+$ T cells (E) in PBMC from patients with stable and active sarcoidosis (n = 8). (F) Proportion of $V_\alpha24^+V_\beta11^+$ NKT cells in lymphocytes in both PBMC and BALF determined in six patients.

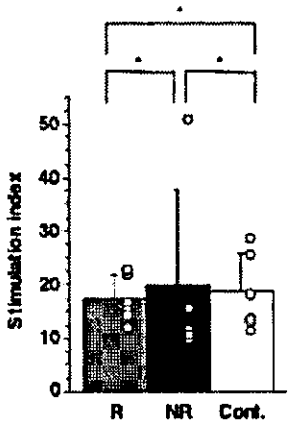

Fig. 4. Evaluation of α-GalCer antigen-presenting ability of patient APC. Murine $V_\alpha14$ NKT cells were cultured with irradiated $CD3^-$ human APC pulsed with α-GalCer or control vehicle. The ^3H uptake of responder NKT cells was measured and the stimulation index calculated. Mean values of remitting (R, $n = 6$) and non-remitting (NR, $n = 5$) sarcoidosis and normal controls (Cont., $n = 6$) are shown with SD; *differences are not significant.

sarcoidosis. Because of limited numbers of $V_\alpha24$ NKT cells in patient samples (see below), we performed a sensitive analysis, semi-quantitative RT-PCR after selective expansion of $V_\alpha24$ NKT cells *in vitro*. PBMC were cultured with IL-2 and α-GalCer (4) to increase $V_\alpha24$ NKT cell numbers, and then FACS-sorted $V_\alpha24^+V_\beta11^+$ double-positive cells were stimulated with PMA and ionomycin to induce potential cytokine production. PCR products of serial dilution of control and experimental samples were hybridized with a $[^{32}P]$dCTP probe, and the intensity of each band quantified by a densitometer. Copy numbers of IFN-γ, IL-4 and GAPDH of experimental samples were estimated by the standard curves obtained in each experiment (Fig. 1C). The levels of IFN-γ mRNA of $V_\alpha24$ NKT cells were revealed to be significantly reduced in patients with non-remitting sarcoidosis compared to those with remitting disease and control samples (Fig. 1A). However, no significant reduction was observed in the levels of IL-4 mRNA among the three groups (Fig. 1B), suggesting a selective dysfunction in T_h1 cytokine (i.e. IFN-γ) production of $V_\alpha24$ NKT cells in patients with non-remitting sarcoidosis.

In order to further investigate whether the dysfunction of IFN-γ production is a specific event in $V_\alpha24$ NKT cells of non-remitting patients, we performed a single-cell RT-PCR analysis. Non-adherent PBMC were stimulated with immobilized anti-CD3 mAb and then $V_\alpha24^+V_\beta11^+$ double-positive cells sorted in a 96-well plate at a single cell per well. Then, $V_\alpha24$ PCR-positive wells were further assayed for IFN-γ gene expression by another RT-PCR. The percentages of IFN-γ-producing cells among $V_\alpha24$ NKT cells in patients with non-remitting and remitting sarcoidosis are shown (Fig. 1D). This single-cell-level analysis demonstrated a significant decrease in the number of IFN-γ-producing $V_\alpha24$ NKT cells in non-remitting sarcoidosis patients as compared to that in remitting patients (Fig. 1D). These results indicate that $V_\alpha24$ NKT cells in non-remitting, but not in remitting, sarcoidosis patients have a decreased potential to produce IFN-γ.

We then investigated cytokine production in conventional CD4 T cells. In contrast to the dysfunction of $V_\alpha24$ NKT cells, CD4 T cells demonstrated normal production of IFN-γ and/or IL-4 in the three groups as demonstrated by an intracellular cytokine staining (Fig. 2). Indeed, no significant difference was detected in the proportion of IFN-γ- (Fig. 2A), IL-4- (Fig. 2B), and IFN-γ/IL-4 double-producing cells (Fig. 2C). The results indicate that cytokine production by CD4 T cells is entirely normal and that the decreased IFN-γ production is therefore specific for $V_\alpha24$ NKT cells in non-remitting sarcoidosis.

Reduced number of $V_\alpha24$ NKT cells in non-remitting sarcoidosis

We also examined the overall number of $V_\alpha24$ NKT cells and $CD3^+$ cells in PBMC of patients with remitting and non-remitting sarcoidosis. The proportion of $V_\alpha24$ NKT cells in the $CD3^+$ population was significantly reduced in patients with non-remitting sarcoidosis compared with that of remitting sarcoidosis and normal controls (Fig. 3A). The absolute number of $V_\alpha24$ NKT cells was also significantly reduced in non-remitting patients (Fig. 3B). In contrast, the percentage of $CD3^+$ T cells of non-remitting sarcoidosis is not significantly different from that of remitting sarcoidosis and normal controls (Fig. 3C). Thus, the reduction of $V_\alpha24$ NKT cell numbers seems to be most prominent in patients with non-remitting sarcoidosis. When paying attention to the disease progress in individual patients, the levels of $V_\alpha24$ NKT cell numbers were lower at the active stage compared to that in the stable stage in all cases (Fig. 3D). However, $CD3^+$ T cell numbers were unchanged in most cases regardless of the disease status (Fig. 3E). When $V_\alpha24$ NKT cell numbers in PBMC were compared with those in BALF of six patients with remitting or non-remitting sarcoidosis, there was a significant correlation in their numbers in PBMC and BALF in all except one patient (Fig. 3F). The results indicate that $V_\alpha24$ NKT cell numbers in PBMC are at a similar level to that in the lung.

Normal APC function in non-remitting sarcoidosis patients

Since the $V_\alpha24$ NKT cell number in patients with non-remitting sarcoidosis was significantly reduced, it is important to investigate whether the reduction is due to a functional defect in either APC or $V_\alpha24$ NKT cells. We thus examined the CD1d-dependent antigen-presenting ability of patient's APC using α-GalCer as a surrogate antigen. $CD3^-$ PBMC were incubated with α-GalCer or control vehicle, irradiated and used as APC. To avoid the influence of variability of $V_\alpha24$ NKT cell numbers in individual patients, we used mouse $V_\alpha14$ NKT cells as responders against patient's APC (19). We found no significant difference observed among the three groups in the ability of patient's APC to stimulate mouse $V_\alpha14$ NKT cells, indicating that these were functioning normally (Fig. 4).

Accumulation of $V_\alpha24$ NKT cells in granuloma lesion of sarcoidosis

We assessed an accumulation of $V_\alpha24$ NKT cells within the granulomas of sarcoidosis by measuring the copy numbers of $V_\alpha24$–$J_\alpha Q$ and C_α gene transcripts by semi-quantitative RT-PCR. We first compared anterior scalene muscle lymph nodes

of pulmonary sarcoidosis patients with hilar lymph nodes of lung cancer patients as a control sample. The proportion of $V_\alpha24$ NKT cells ($V_\alpha24$-$J_\alpha Q$) among total T cells (C_α) was significantly higher in lymph nodes of sarcoidosis than those of lung cancer (Fig. 5A). We also found the proportion of $V_\alpha24$ NKT cells in skeletal muscle granulomas of muscular sarcoidosis patients to be extremely high compared to normal control tissues (Fig. 5B). These data suggest that sarcoidosis

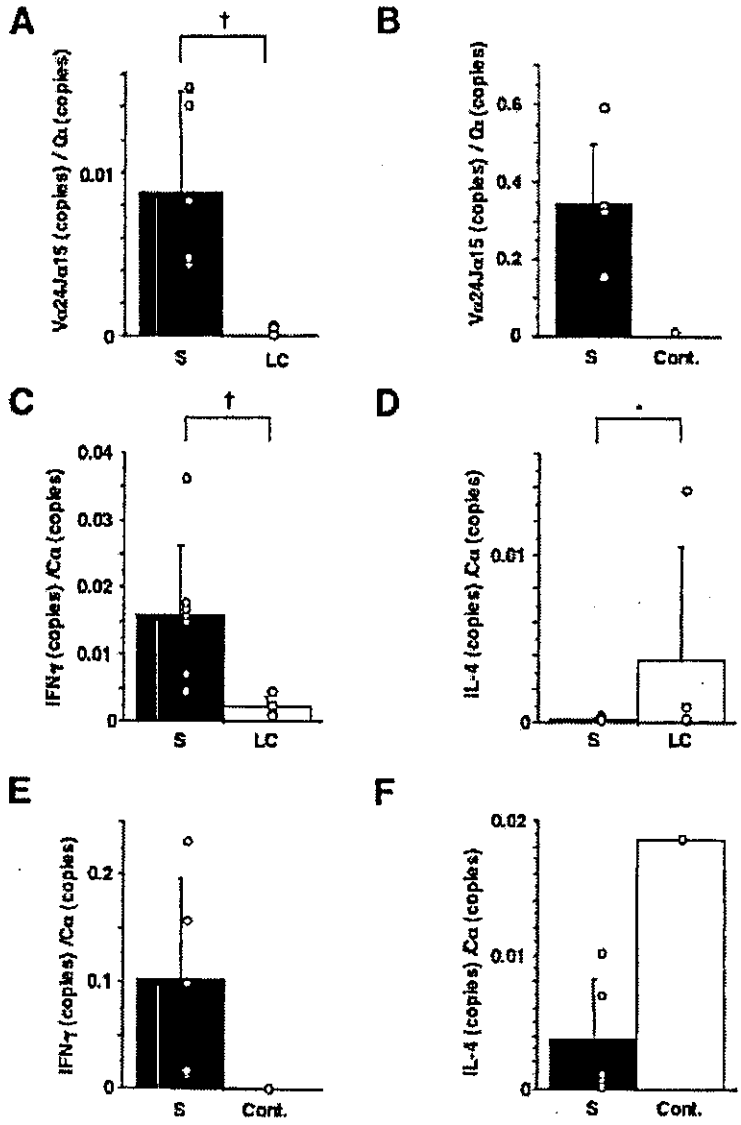

Fig. 5. Accumulation of $V_\alpha24$ NKT cells in granuloma lesions of sarcoidosis. (A) RNA extraction and cDNA synthesis were performed using lymph node samples from sarcoidosis and lung cancer patients. cDNA was subjected to PCR with specific primers for TCR $V_\alpha24$-$J_\alpha Q$ and TCR C_α. PCR products were hybridized with [^{32}P]dCTP-labeled probes. Copy numbers of rearranged $V_\alpha24$-$J_\alpha Q$ DNA compared to C_α in the lymph nodes of pulmonary sarcoidosis (S, $n = 7$: three males, four females, mean age 53.0 ± 8.7 years) and lung cancer (LC, $n = 4$: four samples with no metastasis confirmed; one male, three females, mean age 58.8 ± 14.2 years) patients are shown with SD; †$P < 0.05$. (B) Copy numbers of rearranged $V_\alpha24$-$J_\alpha Q$ DNA compared to total C_α in skeletal muscle granulomas of muscular sarcoidosis patients (S, $n = 5$: two males, three females, mean age 48.8 ± 11.8 years) and normal control (commercially available, Cont., $n = 1$) are shown. (C) and (D) IFN-γ (C) and IL-4 (C) expression in lymph node samples from sarcoidosis and lung cancer patients shown in (A); †$P < 0.05$, *differences are not significant. (E and F) IFN-γ (E) and IL-4 (F) expression in skeletal muscle granulomas of muscular sarcoidosis patients shown in (B). Because only one control sample (a commercial skeletal muscle sample) was used, no statistical study was performed.

involves an accumulation of $V_\alpha24$ NKT cells in granulomatous lesions.

Cytokine expression in granuloma lesion of sarcoidosis

We assessed cytokine expression in the granuloma of sarcoidosis by semi-quantitative RT-PCR. The same samples as Fig. 5(A and B) were used. As shown in Fig. 5(C and D), the expression of IFN-γ is significantly higher in sarcoidosis lymph node granulomas compared to that of lung cancer. As for IL-4, no significant difference was detected. Figure 5(E and F) shows the results with skeletal muscle granulomas of muscular sarcoidosis. A similar increase in IFN-γ expression was detected as compared to normal muscle samples. These results suggest that a substantial amount of IFN-γ expression exists in sarcoidosis granulomas. Since ~100 times more T cells existed in the lymph node granuloma and double the numbers in the muscle granuloma (see Fig. 5A and B, ratios) compared to $V_\alpha24$ NKT cells, the source of IFN-γ would be from T_h1-type T cells as reported (14–16). It is not known about the contribution of $V_\alpha24$ NKT cells to the detected amounts of IFN-γ.

Discussion

Despite the uncertainty regarding etiology, much evidence supports the notion that sarcoidosis involves a severe immunologic dysfunction (12,24). Although $V_\alpha24$ NKT cells are known to produce large amounts of cytokines and control T_h1/T_h2 responses, there have been few reports on their role in the pathogenesis of sarcoidosis in humans. On the other hand, in a murine study, granuloma formation induced by a phosphatidyl inositolmannoside fraction of *M. tuberculosis* was impaired in $V_\alpha14$ NKT cell-deficient ($J_\alpha281^{-/-}$) mice (11), suggesting that $V_\alpha14$ NKT cells play a primary role in the granulomatous responses. Moreover, dysfunction of NKT cells leads to development of autoimmune diseases, such as Type 1 diabetes in NOD mice or experimental encephalomyelitis in mice (25,26). We thus hypothesized that human $V_\alpha24$ NKT cells contribute to the modulation of disease progression and the formation of non-caseating granulomas in sarcoidosis. Here, we found a reduction in both $V_\alpha24$ NKT cell number and IFN-γ production in the PBMC of non-remitting, but not remitting, sarcoidosis patients. These results strongly suggest a role for $V_\alpha24$ NKT cells in the disease progression of sarcoidosis.

The factors that initiate sarcoidosis or modulate its progression have remained unknown. Similarly, it remains impossible to predict whether patients will develop an indolent self-limiting illness or progress to severe tissue destruction. Several pieces of evidence suggest that sarcoidosis is initiated by exposure of genetically susceptible hosts to inhaled environmental agents. Both infectious and non-infectious agents, ranging from simple metals to infectious organisms, have been implicated (17). In this context, it has recently been reported that Gram-positive anerobic bacteria, *Propionibacterium acnes* and *Propionibacterium granulosum*, are probable antigens triggering granuloma formation in sarcoidosis (13).

Elevated expression of T_h1-type cytokines in BALF of sarcoidosis patients and an accumulation of CD4 T cells in granuloma lesions have been reported, suggesting the involvement of T_h1 CD4 T cells in disease pathogenesis (14–16). However, our study revealed that conventional CD4 T cells in the peripheral blood of sarcoidosis patients produced normal (or relatively larger) amounts of IFN-γ compared to those from normal controls (Fig. 2). Thus, the decreased IFN-γ production seemed to be a specific feature of $V_\alpha24$ NKT cells in non-remitting sarcoidosis. Furthermore, the normal levels of IFN-γ production seen in $V_\alpha24$ NKT cells from remitting patients (Fig. 1), together with the accumulation of these cells in granuloma lesions, suggest that IFN-γ production by $V_\alpha24$ NKT cells may control the disease activity. Because IFN-γ produced by NKT cells substantially affects the total T_h1/T_h2 response (27), the dysfunction of $V_\alpha24$ NKT cells in non-remitting patients might lead to an insufficient T_h1 response, resulting in the non-remitting state of the disease.

Mempel *et al.* have reported an absence of $V_\alpha24$ NKT cells in cutaneous lesions of sarcoidosis (28). In contrast, our experiments showed a significant accumulation of $V_\alpha24$ NKT cells in the granuloma lesions of pulmonary and muscular sarcoidosis (Fig. 5). The reason for the discrepancy is unknown, but it may be due to the difference in the stage of sarcoidosis and tissues sampled or the sensitivity of detection of $V_\alpha24$ NKT cells. In this regard, we have recently found that activation of $V_\alpha14$ NKT cells rapidly induces a down-regulation of their $V_\alpha14$ receptor expression (Harada *et al.*, submitted). Thus, it is possible that repeated exposure to unknown pathogens triggers $V_\alpha24$ NKT cells in sarcoidosis patients to down-regulate their receptor expression. The down-regulated $V_\alpha24$ receptor of NKT cells can be detected by PCR, but not by staining with antibody. The use of antibodies or an α-GalCer/CD1d tetramer may therefore fail to detect the existence of $V_\alpha24$ NKT cells.

In any event, the reduced number of $V_\alpha24$ NKT cells and their IFN-γ production appear to be involved in the disease progression of sarcoidosis. A practical benefit of these observations is that analysis of $V_\alpha24$ NKT cell number and function in sarcoidosis may be useful in evaluating disease prognosis. The present findings implicate a new therapeutic strategy for sarcoidosis, such as an activation of $V_\alpha24$ NKT cells with a glycolipid ligand or adoptive transfer of expanded $V_\alpha24$ NKT cells. Further clinical studies are needed to clarify these possibilities.

Acknowledgements

We thank Dr Robert Triendl for reading and Ms Hiroko Tanabe for preparation of this manuscript. This work was supported by the following: Ministry of Education, Culture, Sports, Science and Technology, Japan, Grants-in-Aid for Scientific Research (A) # 13307011 (M. T.), Scientific Research, Priority Areas Research #13218016 (T. N.), Scientific Research B # 14370107 (T. N.), and Special Coordination Funds for Promoting Science and Technology (T. N.), Ministry of Health, Labor and Welfare, Japan, Organization for Pharmaceutical Safety and Research (Project ID #MF-24) (M. T.), Human Frontier Science Program Research Grant (RG00168/2000-M206) (M. T.), and Kirin Brewery Co. Ltd.

Abbreviations

α-GalCer	α-galactosylceramide
APC	antigen-presenting cell

BALF	bronchoalveolar lavage fluid
PBL	peripheral blood lymphocyte
PBMC	peripheral blood mononuclear cell
PE	phycoerythrin
PMA	phorbol 12-myristate 13-acetate

References

1 Taniguchi, M., Harada, M., Kojo, S., Nakayama, T. and Wakao, H. 2003. The regulatory role of $V_\alpha14$ NKT cells in innate and acquired immune response. *Annu. Rev. Immunol.* 21:483.

2 Dellabona, P., Padovan, E., Casorati, G., Brockhaus, M. and Lanzavecchia, A. 1994. An invariant $V_\alpha24$–$J_\alpha Q/V_\beta11$ T cell receptor is expressed in all individuals by clonally expanded CD4-8- T cells. *J. Exp. Med.* 180:1171.

3 Porcelli, S., Yockey, C. E., Brenner, M. B. and Balk, S. P. 1993. Analysis of T cell antigen receptor (TCR) expression by human peripheral blood CD4-8- α/β T cells demonstrates preferential use of several V_α genes and an invariant TCR α chain. *J. Exp. Med.* 178:1.

4 Kawano, T., Cui, J., Koezuka, Y., Toura, I., Kaneko, Y., Motoki, K., Ueno, H., Nakagawa, R., Sato, H., Kondo, E., Koseki, H. and Taniguchi, M. 1997. CD1d-restricted and TCR-mediated activation of $V_\alpha14$ NKT cells by glycosylceramides. *Science* 278:1626.

5 Arase, H., Arase, N., Nakagawa, K., Good, R. A. and Onoe, K. 1993. NK1.1+ CD4+ CD8- thymocytes with specific lymphokine secretion. *Eur. J. Immunol.* 23:307.

6 Chen, H. and Paul, W. E. 1997. Cultured NK1.1- CD4+ T cells produce large amounts of IL-4 and IFN-γ upon activation by anti-CD3 or CD1. *J. Immunol.* 159:2240.

7 Hong, S., Wilson, M. T., Serizawa, I., Wu, L., Singh, N., Naidenko, O. V., Miura, T., Haba, T., Scherer, D. C., Wei, J., Kronenberg, M., Koezuka, Y. and Van Kaer, L. 2001. The natural killer T-cell ligand α-galactosylceramide prevents autoimmune diabetes in non-obese diabetic mice. *Nat. Med.* 7:1052.

8 Sharif, S., Arreaza, G. A., Zucker, P., Mi, Q. S., Sondhi, J., Naidenko, O. V., Kronenberg, M., Koezuka, Y., Delovitch, T. L., Gombert, J. M., Leite-De-Moraes, M., Gouarin, C., Zhu, R., Hameg, A., Nakayama, T., Taniguchi, M., Lepault, F., Lehuen, A., Bach, J. F. and Herbelin, A. 2001. Activation of natural killer T cells by α-galactosylceramide treatment prevents the onset and recurrence of autoimmune Type 1 diabetes. *Nat. Med.* 7:1057.

9 Seino, K., Fukao, K., Muramoto, K., Yanagisawa, K., Takada, Y., Kakuta, S., Iwakura, Y., Van Kaer, L., Takeda, K., Nakayama, T., Taniguchi, M., Bashuda, H., Yagita, H. and Okumura, K. 2001. Requirement for natural killer T (NKT) cells in the induction of allograft tolerance. *Proc. Natl Acad. Sci. USA* 98:2577.

10 Ikehara, Y., Yasunami, Y., Kodama, S., Maki, T., Nakano, M., Nakayama, M., Taniguchi, M. and Ikeda, S. 2000. CD4+ $V_\alpha14$ natural killer T cells are essential for acceptance of rat islet xenografts in mice. *J. Clin. Invest.* 105:1761.

11 Apostolou, I., Takahama, Y., Belmant, C., Kawano, T., Huerre, M., Marchal, G., Cui, J., Taniguchi, M., Nakauchi, H., Fournie, J. J., Kourilsky, P. and Gachelin, G. 1999. Murine natural killer T (NKT) cells contribute to the granulomatous reaction caused by mycobacterial cell walls. *Proc. Natl Acad. Sci. USA* 96:5141.

12 Newman, L. S., Rose, C. S. and Maier, L. A. 1997. Sarcoidosis. *N. Engl. J. Med.* 336:1224.

13 Ishige, I., Usui, Y., Takemura, T. and Eishi, Y. 1999. Quantitative PCR of mycobacterial and propionibacterial DNA in lymph nodes of Japanese patients with sarcoidosis. *Lancet* 354:120.

14 Moller, D. R., Forman, J. D., Liu, M. C., Noble, P. W., Greenlee, B. M., Vyas, P., Holden, D. A., Forrester, J. M., Lazarus, A., Wysocka, M., Trinchieri, G. and Karp, C. 1996. Enhanced expression of IL-12 associated with T_h1 cytokine profiles in active pulmonary sarcoidosis. *J. Immunol.* 156:4952.

15 O'Regan, A. W., Chupp, G. L., Lowry, J. A., Goetschkes, M., Mulligan, N. and Berman, J. S. 1999. Osteopontin is associated with T cells in sarcoid granulomas and has T cell adhesive and cytokine-like properties *in vitro*. *J. Immunol.* 162:1024.

16 Baumer, I., Zissel, G., Schlaak, M. and Muller-Quernheim, J. 1997. T_h1/T_h2 cell distribution in pulmonary sarcoidosis. *Am. J. Respir. Cell. Mol. Biol.* 16:171.

17 Statement on Sarcoidosis. Joint Statement of the American Thoracic Society (ATS), the European Respiratory Society (ERS) and the World Association of Sarcoidosis and Other Granulomatous Disorders (WASOG) adopted by the ATS Board of Directors and by the ERS Executive Committee, February 1999. *Am. J. Respir. Crit. Care Med.* 160:736.

18 Consensus Conference: Activity of Sarcoidosis. Third WASOG meeting, Los Angeles, USA, September 8–11, 1993. *Eur. Respir. J.* 7:624.

19 Kawano, T., Nakayama, T., Kamada, N., Kaneko, Y., Harada, M., Ogura, N., Akutsu, Y., Motohashi, S., Iizasa, T., Endo, H., Fujiwara, T., Shinkai, H. and Taniguchi, M. 1999. Antitumor cytotoxicity mediated by ligand-activated human $V_\alpha24$ NKT cells. *Cancer Res.* 59:5102.

20 Yamashita, M., Kimura, M., Kubo, M., Shimizu, C., Tada, T., Perlmutter, R. M. and Nakayama, T. 1999. T cell antigen receptor-mediated activation of the Ras/mitogen-activated protein kinase pathway controls interleukin 4 receptor function and type-2 helper T cell differentiation. *Proc. Natl Acad. Sci. USA* 96:1024.

21 Kawano, T., Cui, J., Koezuka, Y., Toura, I., Kaneko, Y., Sato, H., Kondo, E., Harada, M., Koseki, H., Nakayama, T., Tanaka, Y. and Taniguchi, M. 1998. Natural killer-like nonspecific tumor cell lysis mediated by specific ligand-activated $V_\alpha14$ NKT cells. *Proc. Natl Acad. Sci. USA* 95:5690.

22 Keino, H., Matsumoto, I., Okada, S., Kurokawa, M., Kato, T., Tokuhisa, T., Usui, M., Taniguchi, M., Nishioka, K. and Sumida, T. 1999. A single cell analysis of TCR AV24AJ18- DN T cells. *Microbiol. Immunol.* 43:577.

23 Makino, Y., Kanno, R., Koseki, H. and Taniguchi, M. 1996. Development of $V_\alpha14^+$ NK T cells in the early stages of embryogenesis. *Proc. Natl Acad. Sci. USA* 93:6516.

24 Agostini, C., Meneghin, A. and Semenzato, G. 2002. T-lymphocytes and cytokines in sarcoidosis. *Curr. Opin. Pulm. Med.* 8:435.

25 Hammond, K. J., Poulton, L. D., Palmisano, L. J., Silveira, P. A., Godfrey, D. I., and Baxter, A. G. 1998. α/β-T cell receptor (TCR)+CD4-CD8- (NKT) thymocytes prevent insulin-dependent diabetes mellitus in nonobese diabetic (NOD)/Lt mice by the influence of interleukin (IL)-4 and/or IL-10. *J. Exp. Med.*187:1047.

26 Singh, A. K., Wilson, M. T., Hong, S., Olivares-Villagomez, D., Du, C., Stanic, A. K., Joyce, S., Sriram, S., Koezuka, Y. and Van Kaer, L. 2001. Natural killer T cell activation protects mice against experimental autoimmune encephalomyelitis. *J. Exp. Med.* 194:1801.

27 Cui, J., Watanabe, N., Kawano, T., Yamashita, M., Kamata, T., Shimizu, C., Kimura, M., Shimizu, E., Koike, J., Koseki, H., Tanaka, Y., Taniguchi, M. and Nakayama, T. 1999. Inhibition of T helper cell type 2 cell differentiation and immunoglobulin E response by ligand-activated $V_\alpha14$ natural killer T cells. *J. Exp. Med.* 190:783.

28 Mempel, M., Flageul, B., Suarez, F., Ronet, C., Dubertret, L., Kourilsky, P., Gachelin, G. and Musette, P. 2000. Comparison of the T cell patterns in leprous and cutaneous sarcoid granulomas. Presence of $V_\alpha24$ invariant natural killer T cells in T-cell-reactive leprosy together with a highly biased T cell receptor V_α repertoire. *Am. J. Pathol.* 157:509.

International Immunology, Vol. 16, No. 2, pp. 241–247
doi: 10.1093/intimm/dxh023

Down-regulation of the invariant Vα14 antigen receptor in NKT cells upon activation

Michishige Harada[1], Ken-ichiro Seino[1,2], Hiroshi Wakao[1], Sakura Sakata[1], Yuko Ishizuka[1], Toshihiro Ito[3], Satoshi Kojo[1], Toshinori Nakayama[3] and Masaru Taniguchi[1]

[1]RIKEN Research Center for Allergy and Immunology, Graduate School of Medicine, Chiba University, Chiba City, Chiba 260-8670, Japan
[2]PRESTO, JST, Kawaguchi City, Saitama 332-0012, Japan
[3]Department of Medical Immunology, Graduate School of Medicine, Chiba University, Chiba City, Chiba 260-8670, Japan

Keywords: α-galactosylceramide, apoptosis, CD1d tetramer, cDNA array, cytokine production

Abstract

NKT cells expressing the invariant Vα14 antigen receptor constitute a novel lymphocyte subpopulation with immunoregulatory functions. Stimulation via their invariant Vα14 receptor with anti-CD3 or a ligand, α-galactosylceramide (α-GalCer), triggers activation of Vα14 NKT cells, resulting in a rapid cytokine production such as IFN-γ and IL-4. Soon after their receptor activation, Vα14 NKT cells disappeared as judged by staining with CD1d tetramer loaded with α-GalCer (α-GalCer/CD1d tetramer), which has been believed to be due to apoptotic cell death. Here we show that such a disappearance was largely attributed to down-regulation of the Vα14 receptor. In fact, Vα14 NKT cells were relatively resistant to apoptosis compared to the conventional T cells as evidenced by less staining with Annexin-V, a limited DNA fragmentation, and their preferential expression of anti-apoptotic genes such as NAIP and MyD118. Furthermore, they did not become tolerant, and maintained their proliferative capacity and cytokine production even after their receptor down-regulation. These as yet unrecognized facets of Vα14 NKT cells are discussed in relation to their regulatory functions.

Introduction

Effector T cells are activated and proliferate to initiate immune responses upon antigen stimulation, whereas in certain milieux, they become anergic or doomed to die by apoptosis (1–3). In contrast, regulatory T cells, such as $CD4^+CD25^+$ cells that mediate immunosuppressive functions, have been shown to be relatively resistant to apoptosis induced by TCR stimulation (4). Moreover, stimulation of a co-receptor molecule, CTLA-4, elicits negative signals and results in the suppression of effector T cell functions, while it leads to the activation of $CD4^+CD25^+$ regulatory T cells (2,5,6). These unique features of effector and regulatory cells can be explained by cell-type-specific outcomes in response to extracellular stimuli, such as TCR engagement and/or cytokines.

Vα14 NKT cells, another type of immunoregulatory cell, possess solely an invariant Vα14 antigen receptor, encoded by Vα14 and Jα281 gene segments, that is reactive to a glycolipid antigen, α-galactosylceramide (α-GalCer), presented by CD1d (7–10). Vα14 NKT cells play crucial immunoregulatory roles in a variety of immune responses, including protection from autoimmune disease development, maintenance of transplantation tolerance and immunological surveillance for tumors [reviewed in (11)]. However, little is known about the molecular events operating in activated Vα14 NKT cells and about the destiny of Vα14 NKT cells upon stimulation. Understanding the comportment of Vα14 NKT cells after activation will help to elucidate the mechanisms

Correspondence to: M. Taniguchi, RIKEN Research Center for Allergy and Immunology, Department of Molecular Immunology, Graduate School of Medicine, Chiba University, 1-8-1 Inohana, Chuo-ku, Chiba 260-8670, Japan. E-mail: mtaniguchi@faculty.chiba-u.jp

Transmitting editor: T. Watanabe
Received 16 September 2003, *accepted* 21 October 2003

through which Vα14 NKT cells exert regulatory functions in the immune system.

In this report we show that Vα14 NKT cell activation results in the rapid down-regulation of the Vα14 receptor. Subsequently, Vα14 NKT cells become undetectable by flow cytometry with α-GalCer/CD1d tetramer staining. Activated Vα14 NKT cells remain quiescent for a while, but eventually proliferate and continue to produce cytokines. Furthermore, these cells show a resistance to apoptosis induced by TCR stimulation relative to conventional T cells. These data indicate that Vα14 NKT cells neither become anergic nor are eradicated by apoptosis upon activation.

Methods

Mice

Eight- to 10-week-old female C57BL/6 mice were from SLC (Hamamatsu, Japan). C57BL/6 Ly-5.1 congenic mice were from Jackson Laboratory (Bar Harbor, ME). All mice were maintained under specific pathogen-free conditions in our animal facility; they were treated in accordance with guidelines for animal care at Chiba University.

Reagents and antibodies

α-GalCer as previously described (10) was kindly provided by Kirin Brewery (Takasaki, Japan). The following mAb were purchased from BD PharMingen (San Diego, CA): anti-CD16/32 (2.4G2) and anti-CD3 (2C11), FITC-conjugated anti-TCRβ (H57-597) and anti-NK1.1 (PK136), and biotin-conjugated anti-TCRβ (H57-597), Ly-5.1 (A20) and Ly-5.2 (104). Anti-FITC microbeads were purchased from Miltenyi Biotec (Auburn, CA). Phycoerythrin-labeled α-GalCer/CD1d tetramer was prepared in our laboratory using a baculovirus expression system kindly provided by Dr M. Kronenberg (La Jolla Institute, La Jolla, CA). Cells were cultured in complete RPMI 1640 medium supplemented with 10% FCS, 2 mM L-glutamine, 100 U/ml penicillin, 100 μg/ml streptomycin and 55 μM 2-mercaptoethanol (Invitrogen, Carlsbad, CA).

Preparation of dendritic cells (DC) and liver mononuclear cells

Mouse splenic DC were prepared as described previously (10). Total liver cells were suspended in a 33% Percoll solution (Pharmacia, Uppsala, Sweden) containing heparin (100 U/ml) and centrifuged at 1000 *g* for 15 min at room temperature. Pellets were used as liver mononuclear cells for subsequent studies after lysing red blood cells.

Stimulation with α-GalCer or α-GalCer-DC

For *in vivo* stimulation, 100 μg/kg of α-GalCer was i.p. injected into mice. For *in vitro* stimulation, DC were pulsed with 100 ng/ml of α-GalCer or vehicle alone for 24 h. After extensive washing, pulsed DC (10×10^3 cells/well) were added to stimulate spleen cells (0.2×10^6 cells/well) cultured in 96-well plates.

Flow cytometric analysis and cell sorting

Single-cell suspensions were prepared in PBS supplemented with 2% FCS and 0.05% sodium azide, pre-incubated with anti-CD16/CD32 mAb to prevent non-specific binding via Fc receptor interactions, and incubated with the appropriate mAb on ice for 30 min. Flow cytometric analysis and cell sorting were performed with Coulter Epics XL or Epics Elite cell sorters (Beckman Coulter, Palo Alto CA). Purity of sorted cells was estimated to be >98%.

Cell labeling with carboxyfluorescein diacetate succinimidyl ester (CFSE)

Electronically sorted Vα14 NKT cells from Ly-5.2 mice liver (10×10^6) were incubated with 1 μM CFSE (Molecular Probes, Eugene, OR) in PBS for 8 min at room temperature. Labeling was stopped by the addition of FCS at equal volume. Labeled cells were washed extensively with medium prior to addition of Ly-5.1$^+$ spleen cells pulsed with α-GalCer or vehicle.

Cytokine concentration measurement by ELISA

Two hundred thousand fresh spleen cells, or spleen cells incubated with α-GalCer-DC for the indicated time periods, were co-cultured for an additional 72 h with α-GalCer-DC or vehicle-DC. At the end of the incubation period, culture supernatants were collected and the concentration of IFN-γ and IL-4 was measured using an ELISA kits (BD PharMingen).

Quantification of genomic DNA by PCR

Genomic DNA was extracted from cells using the QiaAmp DNA blood kit (Qiagen, Hilden, Germany). The amount of amplicons generated during PCR was monitored using the iCycler IQ Detection System (Bio-Rad, Hercules, CA). This method is based on the 5′ to 3′ nuclease activity of Taq polymerase, which allows the release of a fluorescent reporter during the PCR. The sequences of the primers and Taqman probes used in this study were as follows: Vα14: 5′-TGGGAGATACTCAGCAACTCTGG-3′; Jα281: 5′-CAGGTATGACAATCAGCTGAGTCC-3′;TCR Cα exon I forward: 5′-CAGAACCCAGAACCTGCTGT-3′; TCR Cα exon I reverse: 5′-TAGGTGGCGTTGGTCTCTTT-3′; Vα14 probe FAM: 5′-FAM-CACCCTGCTGGATGACACTGCCAC-TAMRA-3′; and TCR Cα exon I-probe FAM: 5′-FAM-CTCCCAAATCAATGTGCCGAAAACCA-TAMRA-3′.

Apoptosis detection assays

Electronically purified T (TCRβ$^+$NK1.1$^-$) and α-GalCer/CD1d tetramer-reactive Vα14 NKT cells (TCRβ$^+$NK1.1$^+$) from liver mononuclear cells were stimulated with plate-bound anti-CD3 mAb (10 μg/ml) for the indicated periods of time. Cells were subsequently stained with FITC-labeled Annexin-V (BD PharMingen) and analyzed with a flow cytometer. DNA fragmentation during apoptosis was monitored using the Cell Death Detection ELISA Plus kit (Roche, Mannheim, Germany).

DNA microarray analysis

Total RNA was prepared from electronically sorted hepatic T and α-GalCer/CD1d tetramer-reactive Vα14 NKT cells stimulated with plate-bound anti-CD3 mAb (10 μg/ml) for 2 h. cDNA was synthesized according to the manufacturer's instructions and labeled antisense RNA was prepared by *in vitro* transcription using T7 RNA polymerase (MessageAmp aRNA kit; Ambion, Austin, TX). Mouse Apoptosis Expression Arrays (R & D Systems, Minneapolis, MN) were used to interrogate the

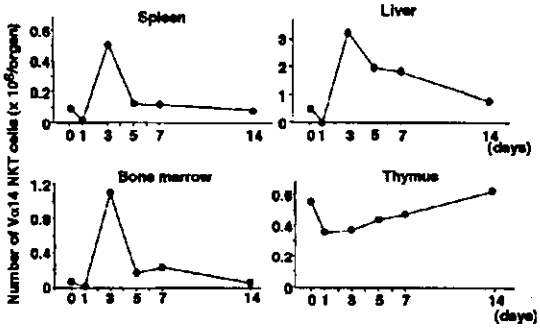

Fig. 1. Kinetics of Vα14 NKT cells from different organs after stimulation with α-GalCer *in vivo*. Mice were injected with α-GalCer (100 μg/kg). After different periods of time, spleen, thymus, liver and bone marrow were removed, and the cells stained with anti-TCRβ and α-GalCer/CD1d tetramer. Absolute numbers of Vα14 NKT cells were calculated from the flow cytometric data. Mean values from three independent mice are indicated.

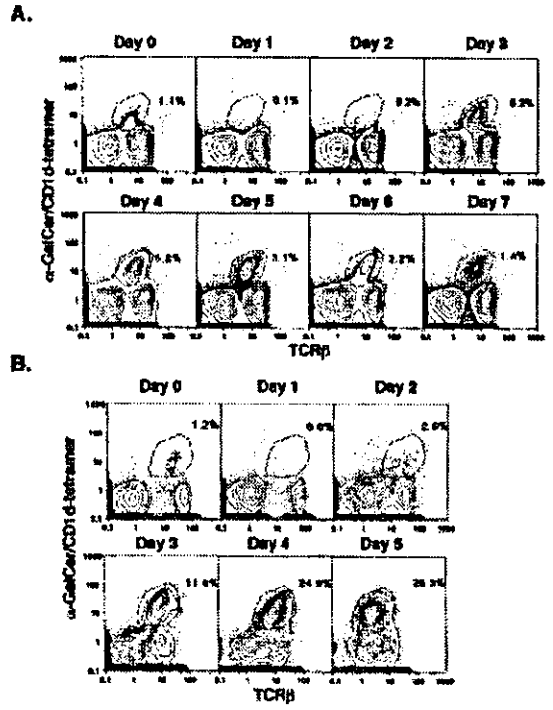

Fig. 2. Comportment of Vα14 NKT cells upon α-GalCer stimulation. (A) Kinetics of disappearance and repopulation of Vα14 NKT cells after α-GalCer stimulation *in vivo*. Spleen cells from C57BL/6 mice before and after administration of α-GalCer (100 μg/kg) were analyzed by flow cytometry at the indicated time. The percentage of Vα14 NKT cells, defined as TCRβ and α-GalCer/CD1d tetramer-reactive cells, is indicated. Representative data from three independent experiments are shown. (B) Kinetics of cell disappearance and repopulation of Vα14 NKT cells after α-GalCer stimulation *in vitro*. Spleen cells from C57BL/6 mice were co-cultured with α-GalCer-DC for the indicated periods of time *in vitro*. Vα14 NKT cells were identified as described in (A). Representative data from three independent experiments are shown.

expression of murine apoptosis-related genes. Radioactive signals were detected with FLA 8000 and the quantitative analysis was performed with Image-Gage software (Fuji Film, Tokyo, Japan).

RT-PCR

cDNA was synthesized from RNA used in DNA microarray analysis with oligo-dT primer. The following primer sets were used for the RT-PCR: NAIP, 5′-TCATGACTGTGCTTGCTTCC-3′ and 5′-CCAGTGGGAACGAACAGTTT-3′; MyD118, 5′-CTC-CTGGTCACGAACTGTCA-3′ and 5′-GGGTAGGGTAGCCTTT-GAGG-3′; IL-1β, 5′-GCCCATCCTCTGTGACTCAT-3′ and 5′-AGGCCACAGGTATTTTGTCG-3′; HPRT, 5′-AGCGTCGTGA-TTAGCGATG-3′ and 5′-CTTTTATGTCCCCCGTTGAC-3′. The number of PCR cycles to detect the above transcripts was as follows: 28 cycles for HPRT, 35 cycles for NAIP, and 37 cycles for MyD118 and IL-1β. PCR products were visualized by ethidium bromide staining and subjected to DNA sequencing to verify authenticity.

Results

Down-regulation of the invariant Vα14 receptors upon activation

To monitor the behavior of Vα14 NKT cells upon receptor activation, α-GalCer was injected i.p. into C57BL/6 mice, and the number of Vα14 NKT cells in the spleen, liver, bone marrow and thymus was examined (Fig. 1). Vα14 NKT cells detected by α-GalCer/CD1d tetramer represented ~1% of the total spleen cells prior to α-GalCer administration (Fig. 2A, day 0). However, the injection of α-GalCer made Vα14 NKT cells virtually undetectable within 24 h (Figs 1 and 2A, *cf.* day 0 and 1, 1.1–0.1%). It was not until day 3 that Vα14 NKT cells robustly reappeared, occupying up to 6.2% of spleen cells. After day 4, the number and proportion of Vα14 NKT cells gradually declined, and reached normal levels by day 14 (Figs 1 and 2A). Such a homeostasis of Vα14 NKT cells after α-GalCer stimulation *in vivo* was also observed in other organs such as liver and bone marrow, but not in the thymus (Fig. 1). Challenging spleen cells with α-GalCer-pulsed DC (α-GalCer-DC) *in vitro* resulted in a similar behavior of Vα14 NKT cells (Fig. 2B), whilst vehicle-pulsed DC (vehicle-DC) had no effect (data not shown). The apparent disappearance of Vα14 NKT cells *in vitro* occurred within 120 min after the addition of α-GalCer-DC (see Supplementary data available at *International Immunology* online). Thus, the receptor-mediated disappearance of Vα14 NKT cells was observed in a manner dependent on an antigen *in vivo* and *in vitro*.

To preclude the possibility that the invariant Vα14 receptor was occupied by α-GalCer on DC and thereby could not be detected by α-GalCer/CD1d tetramer, Vα14 NKT cells were stimulated with plate-bound anti-CD3 mAb and subjected to the same experiments. It turned out that anti-CD3 mAb stimulation also culminated in similar results (see Supplementary data). These data indicate that the apparent disappearance of Vα14 NKT cells was not caused by